

Dynamics of orientational fluctuations of molecules near a liquid-solid interface: A Landau-Ginzburg description

A. Mauger* and D. L. Mills

Department of Physics, University of California, Irvine, California 92715

(Received 5 August 1982)

We present a theory of the frequency spectrum of orientational fluctuations of molecules in a liquid which are near a solid interface at which the molecules are rigidly pinned, with the consequence that there will be orientational order induced in the fluid in the vicinity of the solid interface. It is argued that the fluctuations in orientation in this region may be probed by light scattering spectroscopy, under conditions where the incident light suffers total internal reflection from the boundary. Our theory is based on a time-dependent Landau-Ginzburg equation for the fluctuating part $\delta Q(\vec{x}, t)$ of the orientational-order parameter; the pinning of the molecules at the interface leads to orientational order near the interface, we assume, is described by an order parameter $\bar{Q}(z)$ which falls exponentially as one moves into the liquid. We have carried out a series of calculations of the light scattering spectrum, in the reflection geometry, for the liquid crystal *p*-methoxybenzylidene-*p*-(*n*-butyl)aniline in contact with a dielectric substrate. As the temperature of the nematic-isotropic phase transition is approached from above, pinning of the order parameter can lead to a substantial enhancement in the strength of the central peak in the light scattering spectrum observed in this geometry.

I. INTRODUCTION

In the past few years, light scattering spectroscopy has been employed to study a variety of elementary excitations on solid surfaces, and at interfaces.¹ Raman signals from surfaces are generally weak and hard to detect, though surface polaritons on semiconductors have been studied by this method,² under conditions where there is no substantial enhancement of the electric field of the incident and scattered photon. There have been major advances in Brillouin spectroscopy which allow surface phonons and surface spin waves to be studied in thin films, and in layered media.

Since light scattering signals from liquids can be quite strong, this spectroscopy may prove to be a powerful probe of the dynamics of the liquid state, in the near vicinity of an interface with a solid. Such studies may be carried out in the geometry illustrated in Fig. 1. One has a liquid with dielectric constant ϵ_L placed over a nominally transparent dielectric substrate with dielectric constant ϵ_s , and $\epsilon_s > \epsilon_L$. The incident photon thus has a field which decays exponentially as one moves into the liquid,³ if its angle of incidence is greater than the critical angle θ_c and as a consequence the wave serves as a probe of the near vicinity of the interface. In the scattering experiment, the scattered photon can also exist with angle to the normal, θ_s , greater than the

critical angle θ_c . Thus both photons have fields localized near the interface. For typical liquid-solid interfaces, one estimates the penetration depth of the fields to be in the range of a few hundred angstroms. In this geometry, Dil and van Hijningen have explored the Brillouin spectrum produced by density fluctuations in a liquid in the vicinity of a solid interface.⁴

In addition to the phononlike features produced by scattering from density fluctuations, the light scattering spectrum of a liquid contains a central peak dominated by scattering from fluctuations in molecular orientation, in fluids of complex molecules. While the liquid may be isotropic on the time average, dynamic fluctuations produce local orientational order which subsequently decays in a characteristic time. This leads to a central peak in the light scattering spectrum. This paper explores the way in which the frequency spectrum of such orientational fluctuations can be affected by the proximity of molecules to a solid interface.

The basic notion is the following. While the liquid may be isotropic, right at the interface with the solid, the molecules can in general be assumed to be oriented in some fashion. If the correlation length associated with orientational fluctuations is ξ , the orientational order forced upon the liquid at the boundary will extend a distance the order of ξ into the fluid. In this "selvedge region" between the

solid and the isotropic bulk fluid, the frequency spectrum of the orientational fluctuations may differ substantially from those in the bulk fluid, and the light scattering method outlined earlier, at least in principle,⁵ can serve as a probe of those differences. Liquid crystals should prove to be of particular interest, because near the phase transition (weakly first order) from the isotropic to the nematic phase, the correlation length ξ becomes quite large, comparable in magnitude to the optical penetration depth into the fluid. Furthermore, from a good experimental study⁶ of the liquid crystal pentylcyano-biphenyl (5CB) in contact with a solid substrate [hexadecyltrimethylammonium bromide (HTAB)], it is clear that orientational order is indeed present near the interface, and extends over a region with spatial extent that increases dramatically as the transition to the nematic phase is approached from above.

The aim of this paper is to develop a model description of the influence of a solid boundary on orientational fluctuations in liquids in the vicinity of a solid boundary, and then explore the behavior of the light scattering spectrum, when the back-scattering geometry in Fig. 1 is employed. We have developed a simple-model description of these fluctuations, based on a continuum theory where the Landau free energy is expanded as a power series in the order parameter, and a time-dependent Landau-Ginzburg description is employed for the dynamics. The basic approach is thus a generalization of the methods which have been found to provide an excellent description of the physics of bulk liquid crystals though, as the reader shall appreciate, it will be necessary for us to introduce simplifications at various stages, to keep the analysis tractable.

While our primary emphasis is on the dynamics of liquid crystals in the vicinity of an interface which provides orientational pinning, the basic model may be applied in other physical situations where a surface or interface induces order. For example, Höchli and Rohrer⁷ have argued that in SrTiO₃, the surface induces a low symmetry phase of D_{4h} symmetry, at temperatures above the bulk transition temperature. The approach used here may also provide a Landau-Ginzburg description of the dynamics of this spatially inhomogeneous phase; in this system, the light scattering method discussed here may not prove to be a suitable probe, but surface acoustic-wave attenuation may offer access to the dynamics of the surface region.

In the model presented here a Green's-function method is used to determine the frequency spectrum of thermal orientational fluctuations in the liquid near the surface. By the Kubo or fluctuation-dissipation theorem, this information enables us to

construct the response of the surface region to the external electric field of the electromagnetic wave. Numerical applications are made for the particular case of *p*-methoxybenzylidene-*p*-(*n*-butyl)aniline (MBBA) because many experiments have been performed on this particular liquid crystal, which provide us with the experimental values of all the bulk parameters required for such calculations.

The two main parameters which determine the scattering efficiency are the temperature and the angle of incidence of the light on the surface. The reason is that the temperature determines the correlation length, while the angle of incidence determines the penetration depth of the light inside the liquid crystal.

The outline of the paper is as follows: In Section II, we present a Green's-function description of light scattering by the orientational fluctuations near the surface. In Sec. III the response of the molecules of the liquid crystal close to the surface is derived in the time-dependent Landau-Ginzburg formalism. In Sec. IV, the calculation of the correlation function is presented in the limit of a small order parameter at the surface, which is a simple case that allows one to discuss the frequency dependence of the spectral density. This special limit incorporates a number of features present in the general spectrum. In Sec. V, the Green's function associated with the thermal fluctuations and the scattered light intensity is derived in the general case, while the numerical applications are reported in Sec. VI. In Sec. VII, the results are discussed and analyzed. It is shown in particular that the results can be simply interpreted by introducing at the surface an effective potential of the Morse form, which admits one stable bound state.

II. LIGHT SCATTERING FROM ORDER-PARAMETER FLUCTUATIONS IN THE REFLECTION GEOMETRY

We shall begin with a summary of the theory of light scattering geometry illustrated in Fig. 1. Our aim is not to provide a complete description of this phenomenon for a general scattering configuration, but rather to carry the discussion through to the point where it is clear what correlation function is probed in such studies.

Following de Gennes,⁸ we describe the liquid crystal by the order parameter

$$Q_{\alpha\beta} = \frac{3}{2}(\hat{n}_\alpha \hat{n}_\beta - \frac{1}{3}\delta_{\alpha\beta}), \quad (2.1)$$

where $\hat{n}(\vec{x})$, the director, is a vector that describes the net alignment of the molecules in the fluid. At temperatures above the transition to the nematic phase, the time average $\langle Q_{\alpha\beta} \rangle$ of each component

of the order parameter vanishes. Near the interface, however, all the components of the tensor $\langle Q_{\alpha\beta} \rangle$ do not vanish when the wall imposes some orientation of the molecules of the liquid crystal, which is the common experimental situation.^{6,8} For simplicity, let us consider the case of the pinning at a liquid-solid interface where the fluid retains the cylindrical symmetry about the z axis in Fig. 1. From an experimental point of view, this is the configuration met, for example, in homotropic textures where the easy axis is perpendicular to the surface. In that case, near the interface, we can write

$$\langle Q_{xx} \rangle = \langle Q_{yy} \rangle = -\frac{1}{2} \langle Q_{zz} \rangle = Q(z), \quad (2.2)$$

where $Q(z)$ will decay to zero as one moves into the fluid. There will be fluctuations $\delta Q_{\alpha\beta}(\vec{x}, t)$ in the parameter not only near the interface, but also in the fluid, and these fluctuations modulate the dielectric constant $\epsilon_{\alpha\beta}$ of the fluid, to produce light scattering. We have, separating the dielectric tensor into a static part $\bar{\epsilon}_{\alpha\beta}(z)$ and a fluctuating part $\delta\epsilon_{\alpha\beta}(\vec{x}, t)$,

$$\epsilon_{\alpha\beta} = \bar{\epsilon}_{\alpha\beta}(z) + \delta\epsilon_{\alpha\beta}(\vec{x}, t), \quad (2.3)$$

where

$$\delta\epsilon_{\alpha\beta}(\vec{x}, t) = \sum_{\gamma, \delta} \Gamma_{\alpha\beta; \gamma\delta} \delta Q_{\gamma\delta}(\vec{x}, t). \quad (2.4)$$

If light propagates in the fluid, one may obtain descriptions of the inelastic scattering produced by the fluctuations by solving the Maxwell equations¹

$$[\vec{\nabla} \times (\vec{\nabla} \times \vec{E})]_{\alpha} - \epsilon_0(z) \frac{\Omega^2}{c^2} E_{\alpha} = \frac{\Omega^2}{c^2} \sum_{\beta} \delta\epsilon_{\alpha\beta} E_{\beta}, \quad (2.5)$$

where Ω is the frequency of the light and $\epsilon_0(z)$ the static dielectric constant of the structure in Fig. 1, i.e., $\epsilon_0(z)$ equals the dielectric constant ϵ_s of the solid for $z < 0$, and that ϵ_L of the liquid (assumed isotropic) for $z > 0$. Here c is the light velocity in the vacuum. In principle, the static order induced near the solid-liquid interface, as described by Eq. (2.2), will lead to spatial modulations of the static piece $\epsilon_{\alpha\beta}(z)$ of the dielectric tensor. We ignore these terms with our use of the simple form of $\epsilon_0(z)$, since they will only lead to small modification of the field profiles of the incident and scattered photons near the interface.

The geometry illustrated in Fig. 1, where the incident beam, the scattered beam, and the normal to the interface all lie in one plane, is particularly simple. If we suppose further that the incident and scattered light is s polarized (\vec{E} parallel to \hat{y}), only $\delta\epsilon_{yy}$ enters. Then the only nonzero coupling constants which enter Eq. (2.4) are $\Gamma_{yy;xx}$, $\Gamma_{yy;yy}$, and $\Gamma_{yy;zz}$, so in this geometry one couples to fluctua-

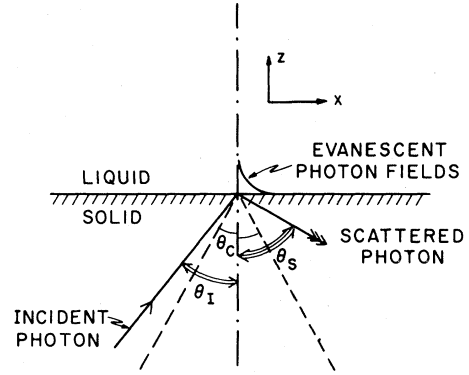


FIG. 1. Scattering geometry which forms the basis for the discussion in the present paper. A photon strikes the liquid-solid interface at an angle θ_c , as its field penetrates only a short distance into the liquid. Similarly, the scattered photon emerges with angle greater than θ_c , as its field is also localized near the interface. \vec{x} is in the plane of incidence.

tions in only the diagonal elements of the order parameter. One may remark that the experimental work of Dil and van Hijningen¹⁴ shows that scattering from fluctuations in the liquid are in fact strong enough to detect, unobscured by signals from the substrate.

We now introduce one assumption not particularly crucial to the presentation, but which will greatly simplify the subsequent discussion. This is that the dominant fluctuations near the interface have the same symmetry as the static order parameter itself, so $\delta Q_{xx} = \delta Q_{yy} = -\frac{1}{2} \delta Q_{zz} \equiv \delta Q(\vec{x}, t)$. This reduces the problem to the study of a single fluctuating coordinate, in the presence of the inhomogeneity near the interface. We are exploring the possibility of incorporating fluctuations of lower symmetry in the analysis, and the present model is the simplest picture which includes the physics we believe essential to the problem. We may then write

$$\delta\epsilon_{yy} = \left[\frac{\partial \epsilon}{\partial Q} \right] \delta Q(\vec{x}, t). \quad (2.6)$$

It is possible to estimate the magnitude of the coupling constant $(\partial\epsilon/\partial Q)$ in Eq. (2.6), from data on the anisotropy of the refractive indices $n_{||} - n_{\perp}$ in the nematic phase of the liquid crystal. Measurements on the material MBBA show that $n_{||} - n_{\perp}$ varies linearly with the order parameter Q in the nematic phase, even when Q is 0.4 or larger.⁹ From this data, and Eq. (2.6) with $\delta Q(\vec{x}, t)$ replaced by the static order parameter Q , we estimate $(\partial\epsilon/\partial Q) \simeq 1.0$.

One may solve the differential equations for the scattered fields in the substrate by using a matrix of

Green's functions for the Maxwell equation. These satisfy, for the case where the scattering is quasielastic

$$\sum_{\lambda} \left[[\vec{\nabla} \times (\vec{\nabla} \times)]_{\alpha\lambda} - \delta_{\alpha\lambda} \epsilon_0(z) \frac{\Omega^2}{c^2} \right] G_{\lambda\beta}(\vec{x}, \vec{x}'; t - t') = \delta_{\alpha\beta} \delta(\vec{x} - \vec{x}') \delta(t - t'), \quad (2.7)$$

where in the present geometry these may be Fourier transformed as follows:

$$G_{\alpha\beta}(\vec{x}, \vec{x}'; t - t') = \int \frac{d^2 k_{||} d\Omega}{(2\pi)^3} e^{i\vec{k}_{||} \cdot (\vec{x}_{||} - \vec{x}'_{||})} \times e^{-i\Omega(t-t')} G_{\alpha\beta}(\vec{k}_{||}, \Omega; z, z'), \quad (2.8)$$

where the subscript $||$ denotes a vector (or com-

$$E^{(s)}(\vec{x}, t) = \frac{\Omega^2}{c^2} \left[\frac{\partial \epsilon}{\partial Q} \right] \int_{-\infty}^{+\infty} dt' \int_{z' > 0} G_{yy}(\vec{x}, \vec{x}'; t - t') \delta Q(\vec{x}', t') E_0(\vec{x}', t'), \quad (2.11)$$

with $E_0(\vec{x}', t')$ the electric field of the incident photon in the liquid. This expression is valid only in the first Born approximation, which is valid here since the intensity of inelastically scattered light is, at best, very weak. If T is the transmission coefficient of the field through the interface, and $E^{(0)}$ its amplitude in the substrate, then

$$E_0 = E^{(0)} T \exp(i\vec{k}_{||}^{(0)} \cdot \vec{x}'_{||}) \exp(-\gamma_0^{(0)} z'). \quad (2.12)$$

The upper index on $\gamma_0^{(0)}$ has been added to distinguish this parameter given by Eq. (2.10) with θ equal to the angle of incidence of the light θ_I , from the extinction coefficient $\gamma_0^{(s)}$ for the scattered photon, given by Eq. (2.10) with θ equal to the angle of emergence θ_s , of the scattered light in the substrate.

We can now calculate the scattered light intensity I from Eqs. (2.8)–(2.12). When the scattering angle θ_s is greater than the critical angle of total internal reflection θ_c , illustrated in Fig. 1 ($\gamma_0^{(0)}$ and $\gamma_0^{(s)}$ are real), one has

$$I = |E^s|^2 = \left[\frac{\Omega}{c} \right]^4 |E_0|^2 |T|^2 \left[\frac{\partial \epsilon}{\partial Q} \right]^2 \int \frac{d^2 k_{||}^{(s)} d\omega}{(2\pi)^3} \frac{1}{|\gamma_0^{(s)} + ik_z^{(s)}|^2} \times \int d^2 x_{||} e^{i\vec{q}_{||} \cdot \vec{x}_{||}} \int_0^{\infty} dz \int_0^{\infty} dz' e^{-\gamma(z+z')} \langle \delta Q(\vec{0}, z) \delta Q(\vec{x}_{||}, z') \rangle_{\omega} \quad (2.13)$$

where $\vec{q}_{||} = \vec{k}_{||}^{(s)} - \vec{k}_{||}^{(0)}$ is the difference in wave vector of the incident and scattered photon, projected onto the plane of the interface. Also, ω is the frequency shift of the scattered light, and $\gamma = \gamma_0^{(0)} + \gamma_0^{(s)}$, with $\gamma_0^{(0)}$ and $\gamma_0^{(s)}$ the extinction coefficients of the incident and scattered light in the liquid as discussed above. In Eq. (2.13), the angular brackets denote a thermodynamic average, and

$$\langle \delta Q(\vec{0}, z) \delta Q(\vec{x}_{||}, z') \rangle_{\omega} = \int_{-\infty}^{+\infty} dt e^{i\omega t} \langle \delta Q(\vec{0}, z; 0) \delta Q(\vec{x}_{||}, z'; t) \rangle. \quad (2.14)$$

It is now straightforward to evaluate the fraction of the light scattered, per unit solid angle, per unit frequency range. We have for this quantity \mathcal{E}

$$\mathcal{E} = \frac{1}{|E_0|^2} \frac{d^2 I}{d\omega d\Omega_s}, \quad (2.15)$$

ponent of a vector) in the plane parallel to the interface. For the two-layer geometry of present interest, these functions may be found in the literature.¹⁰ We need only $G_{yy}(\vec{k}_{||}, \Omega; z, z')$ in the present application, for $z' > 0$ and $z < 0$. This function has the form

$$G_{yy}(\vec{k}_{||}, \Omega; z, z') = \frac{e^{ik_z z} e^{-\gamma_0^{(s)} z'}}{\gamma_0^{(s)} + ik_z}, \quad (2.9)$$

where for a wave incident on the interface, with the angle of incidence $\theta = \theta_s$, the quantity

$$\gamma_0 = \frac{\Omega}{c} (\epsilon_s \sin^2 \theta - \epsilon_L)^{1/2} \quad (2.10)$$

is the inverse of the penetration depth of the electromagnetic field into the liquid, and k_z is the z component of the wave vector of the wave in the substrate.

The scattered electric field may then be written

with $d\Omega_s$ the solid angle, and we also have the differential relationship

$$\frac{d^2 k_{||}^{(s)}}{d\Omega_s} = \epsilon_s \frac{\Omega^2}{c^2} \cos \theta_s, \quad (2.16)$$

which may be derived from the Jacobian of the

transformation between $\vec{k}_{||}^{(s)}$ and the polar angles θ_s and φ_s that specify the direction of the scattered beam.

The transmission coefficient T which appears is simply the appropriate Fresnel coefficient, which may be written

$$T = \frac{2\gamma^{(0)}}{\gamma^{(0)} + ik_z^{(0)}} \quad (2.17)$$

with $k_z^{(0)}$ the z component of wave vector of the incident light in the substrate.

After some algebra, the scattering efficiency per unit solid angle per unit frequency may be written

$$\begin{aligned} \mathcal{E} &= \frac{\cos\theta_s}{2\pi^3} \frac{\epsilon_s}{\epsilon_L} \left[\frac{\partial\epsilon}{\partial Q} \right]^2 \left[\frac{\sin^2\theta_I - \sin^2\theta_c}{\cos^4\theta_c} \right] \\ &\times \left[\frac{\Omega}{c} \right]^4 \mathcal{F}(\vec{q}_{||}, \omega), \end{aligned} \quad (2.18)$$

where

$$\begin{aligned} \mathcal{F}(\vec{q}_{||}, \omega) &= \int d^2x_{||} e^{i\vec{q}_{||} \cdot \vec{x}_{||}} \\ &\times \int_0^\infty dz \int_0^\infty dz' e^{-\gamma(z+z')} \\ &\times \langle \delta Q(\vec{0}, z) \delta Q(\vec{x}_{||}, z') \rangle_\omega. \end{aligned} \quad (2.19)$$

The last step is to break down the spectrum of fluctuations into spatial Fourier components parallel to the interface. We shall see that, for parameters of interest to us, we can neglect the $\vec{q}_{||}$ dependence of $\mathcal{F}(\vec{q}_{||}, \omega)$. This implies that the Fourier transform $\mathcal{F}(\vec{x}_{||}, \omega)$ falls off rapidly with $\vec{x}_{||}$, and thus may be approximated, by a Dirac function $\delta(\vec{x}_{||})$, or, according to Eq. (2.19):

$$\langle \delta Q(\vec{0}, z) \delta Q(\vec{x}_{||}, z') \rangle_\omega = \langle \delta Q(z) \delta Q(z') \rangle_\omega \mathcal{A} \delta(\vec{x}_{||}), \quad (2.20)$$

where \mathcal{A} is a quantization area which we shall take as unity, and we have written

$$\langle \delta Q(z) \delta Q(z') \rangle = \langle \delta Q(\vec{0}, z) \delta Q(\vec{0}, z') \rangle_\omega. \quad (2.21)$$

It follows that the neglect of the $\vec{q}_{||}$ dependence of $\mathcal{F}(\vec{q}_{||}, \omega)$ amounts to neglecting correlations of orientational motions in the xy plane. We shall return to this point later. Then we are reduced to a one-dimensional problem, with

$$\begin{aligned} \mathcal{F}(\vec{q}_{||}, \omega) &\cong \mathcal{F}(\omega) \\ &= \int_0^\infty dz \int_0^\infty dz' e^{-\gamma(z+z')} \\ &\times \langle \delta Q(z) \delta Q(z') \rangle_\omega. \end{aligned} \quad (2.22)$$

III. THE DESCRIPTION OF THE NEAR VICINITY OF THE BOUNDARY

As in the preceding section, we consider the liquid crystal described by the scalar order parameter Q , and for the moment we suppose it depends possibly on the time, and only on the coordinate z normal to the surface. For the purpose of contact with light scattering studies, we shall see that the latter assumption is well justified. The very first monolayer of molecules is supposed tightly bonded to the solid surface, and our attention is directed to the fluid outside this layer within which orientational order is induced.

The Landau–de Gennes free-energy density may be written¹¹

$$\begin{aligned} F &= \frac{1}{2} A(T) Q^2 - \frac{1}{3} B Q^3 + \frac{1}{4} C Q^4 + \frac{1}{2} D \left[\frac{\partial Q}{\partial z} \right]^2 \\ &+ V_0 \delta(z) Q, \end{aligned} \quad (3.1)$$

where in the model, the coefficient $A(T)$ is taken to be

$$A(T) = a_L (T - T^*). \quad (3.2)$$

If the coefficient B were zero, the system would undergo a second-order transition to the nematic phase at $T = T^*$. However, the cubic term in Eq. (3.1) does not vanish,⁸ which means that the isotropic-nematic phase transition is a first-order transition at $T_c = T^* + 2B^2/3a_L C$. At T_c , the order parameter jumps discontinuously from 0 to $Q_c = 2B/3C$. The next to last term is the deformation energy, which is approximated by the simple form displayed in Eq. (3.1). This form is used commonly in the literature on liquid crystals^{6,12} although the full form of the deformation energy is more complex.¹³ Finally, the last term in Eq. (3.1) represents the pinning force exerted on the molecules in the liquid, by the layer tightly bound to the substrate.

Within the framework of a time-dependent Landau-Ginzburg description, the time variation of the order parameter is given by¹⁴

$$\nu \frac{\partial Q}{\partial t} + 2\mu A_s = - \frac{\partial F}{\partial Q}. \quad (3.3)$$

Here ν and μ are viscositylike coefficients, and A_s is the shear rate tensor. In the regime of frequency and wave vector of interest to light scattering (small wave vectors), the hydrodynamic motions which contribute to A_s are slow compared with those of Q , so that the influence of the shear rate tensor is negligible.⁸ We thus drop this term, and Eq. (3.3) then becomes

$$A(T)Q - BQ^2 + CQ^3 - D \frac{\partial^2 Q}{\partial z^2} + \nu \frac{\partial Q}{\partial t} = \mathcal{F}, \quad (3.4)$$

where $\mathcal{F} = \mathcal{F}_s + \delta\mathcal{F}$ with $\mathcal{F}_s = V_0\delta(z)$ the pinning force. We have added a second driving term for Q , $\delta\mathcal{F}(z,t)$, whose precise form we shall not require. We then write $Q(z,t) = \bar{Q}(z) + \delta Q(z,t)$ and separate Eq. (3.4) into a time-independent and time-dependent piece, and we then linearize the time-dependent portion with respect to $\delta Q(z,t)$. The time-independent portion determines the static profile $\bar{Q}(z)$:

$$A\bar{Q} - B\bar{Q}^2 + C\bar{Q}^3 - D\frac{\partial^2\bar{Q}}{\partial z^2} = V_0\delta(z), \quad (3.5)$$

while the time-dependent fluctuations are controlled by

$$\begin{aligned} v\delta\dot{Q} + A(T)\delta Q - 2B\bar{Q}(z)\delta Q + 3C[\bar{Q}(z)]^2\delta Q \\ - D\frac{\partial^2}{\partial z^2}\delta Q = \delta\mathcal{F}(z,t). \end{aligned} \quad (3.6)$$

A. Static effects

Over most of the "selvedge region" within which $\bar{Q}(z)$ is nonvanishing, $\bar{Q}(z)$ will not be large, and the \bar{Q}^2 and \bar{Q}^3 terms in Eq. (3.5) will have a modest influence. If we ignore these, then Eq. (3.5) is readily solved to yield

$$\bar{Q}(z) = Q_0 \exp(-z/\xi), \quad (3.7)$$

where $\xi = (D/A)^{1/2} = \{D/[a_L(T-T^*)]^{1/2}\}$, and $Q_0 = V_0/[2(AD)^{1/2}]$. The correlation length ξ can be quite large. For MBBA, $\xi \approx 200$ Å, when $T = T_c$, the temperature of the first-order phase transition. Note that Q_0 , the magnitude of the order parameter close to the solid, grows with temperature as T_c is approached from above.

We are now in a position to compare our model of $\bar{Q}(z)$ with the data reported by Miyano.⁶ First notice that as the temperature is increased well above T_c , the birefringence does not vanish, but decreases substantially to assume a temperature-independent value. In our picture, this residual effect has its origin in the first monolayer, bound to the surface so tightly that it remains oriented well above T_c . The strongly temperature-dependent excess birefringence which sets in as the temperature is lowered has its origin in the fluid outside this innermost solid layer. Miyano argues that this is controlled by $\int_0^\infty dz \bar{Q}(z)$, which in our model should vary with temperature as $(T-T^*)^{-1}$, when the temperature variation of Q_0 is noted. We have subtracted the background pro-

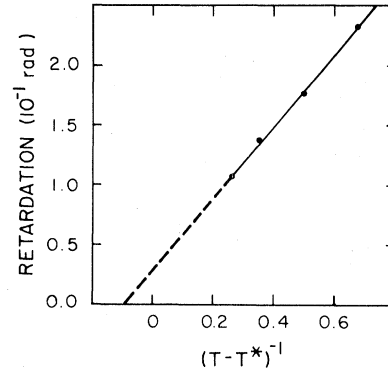


FIG. 2. We plot the signal observed by Miyano (Ref. 6) as a function of $(T-T^*)^{-1}$, after the background signal has been subtracted off, as described in the text. One sees, the linear variation with $(T-T^*)^{-1}$, as expected from our model.

duced by the solid layer from the total amount of birefringence, then inverted the results and plotted the inverse as a function of temperature in Fig. 2. We indeed find a straight line, with a small negative intercept. This suggests our model of $\bar{Q}(z)$ is reasonable. There may be some uncertainty in Miyano's assignment of the value of T^* , due to the fact that his T^* was calculated rather than experimentally determined. In another study, Lister and Stensen¹⁵ experimentally determined T_c and T^* in MBBA. There is in fact a variation of $T_c - T^*$ from sample to sample. This difference may range from 0.8 to 1.2 K, so any uncertainty in a calculated value of T^* can be in the range of ± 0.2 K. Since a shift of T^* by 0.1 K is sufficient to eliminate the negative intercept in Fig. 2, we do not regard this discrepancy between our model and the data as serious.

B. Dynamic fluctuations near the interface above T_c —general remarks

In Eq. (3.7), we give the equation which describes time and spatial variations of the order parameter produced by coupling the system to an external force. From the fluctuation-dissipation theorem, we know the Green's function associated with this differential equation may be used to generate the frequency spectrum of the fluctuations probed by the light scattering method. Thus we are led to introduce the Green's function $G(z,z';t-t')$ which is the solution of

$$\left[v\frac{\partial}{\partial t} + A - 2B\bar{Q}(z) + 3C[\bar{Q}(z)]^2 - D\frac{\partial^2}{\partial z^2} \right] G(z,z';t-t') = \delta(z-z')\delta(t-t'). \quad (3.8)$$

From Sec. II, we see that we require the time Fourier transform of this equation, which takes the form

$$\left[A - i\omega\nu - 2BQ_0 e^{-z/\xi} + 3CQ_0^2 e^{-2z/\xi} - D \frac{\partial^2}{\partial z^2} \right] G(z, z'; \omega) = \delta(z - z'). \quad (3.9)$$

The quantity $\langle \delta Q(z) \delta Q(z') \rangle_\omega$ which enters the light scattering cross section in Eq. (2.22) is then correlated to the Green's function by the fluctuation-dissipation theorem.¹⁶ Since we shall always be interested in frequencies so low that $\hbar\omega \ll k_B T$, only the classical form of the fluctuation-dissipation theorem need be used. We then have

$$\langle \delta Q(z) \delta Q(z') \rangle_\omega = \frac{2k_B T}{\omega} \text{Im} G(z, z'; \omega). \quad (3.10)$$

Let us define the quantity \mathcal{S} by the relation

$$\mathcal{S}(\omega) = \frac{k_B T}{\omega} \int_0^\infty dz \int_0^\infty dz' e^{-\eta(z+z')} G(z, z'; \omega). \quad (3.11)$$

According to Eqs. (2.16)–(2.22), the imaginary part of \mathcal{S} ,

$$S = \text{Im}[\mathcal{S}(\omega)], \quad (3.12)$$

gives the Brillouin scattering efficiency \mathcal{E} , except for a scaling factor independent of Q_0 , ω , and T . The quantity $\mathcal{S}(\omega)$ defined in Eq. (2.22) is equal to $2S$.

Equation (3.9) is not by itself sufficient to determine the form of the Green's function. The differential equation must be supplemented by suitable boundary conditions. If z' is held fixed at a finite value, then since fluctuations are correlated over only a finite distance, quite clearly we must have

$$\lim_{z \rightarrow \infty} G(z, z'; \omega) = 0 \quad (3.13a)$$

If z is fixed, a similar statement applies to the behavior of $G(z, z'; \omega)$ considered as a function of z' .

Now as argued above, we expect the first monolayer of liquid-crystal molecules to be tightly bonded to the substrate, and this implies orientational fluctuations in the near vicinity of this layer will be strongly suppressed. In essence, we require $\delta Q(z, t)$ to vanish as $z \rightarrow 0$ as a consequence, and for fixed z' this translates into a second boundary on $G(z, z'; \omega)$;

$$\lim_{z \rightarrow 0} G(0; z'; \omega) = 0. \quad (3.13b)$$

A similar boundary condition applies to the z' variation of the Green's function, if z is held fixed. There would be no great difficulty carrying through the analysis presented below with a more general boundary condition, in which a linear combination of $\delta Q(z, t)$ and $\partial \delta Q / \partial z$ were required to vanish at $z = 0$. Such a boundary condition would then intro-

duce an additional parameter into the analysis. We believe the boundary condition in Eq. (3.13b) is quite reasonable from the physical point of view, and in the absence of data we see little reason to complicate the discussion in this fashion, at the present time.

The next step is to carry out explicit construction of the Green's function, then evaluate the integral on z and z' in Eq. (2.22). We first consider the case $Q_0 = 0$, where the solution may be expressed entirely in terms of elementary functions. Then we turn to the general case with $Q_0 \neq 0$ and arbitrary in value. The special case $Q_0 \equiv 0$ is worth consideration, since a number of features in the spectrum produced by the full theory do not depend on Q_0 and are contained in this special case.

IV. AN ASYMPTOTIC LIMIT; THE CASE $Q_0 \equiv 0$

At first sight, to take the limit $Q_0 \rightarrow 0$ seems not reasonable, since the whole point of the present analysis is to explore the influence of orientational order near the surface on the light scattering spectrum. By studying this special case, and comparing the behavior of the spectrum when $Q_0 \equiv 0$ with the general case in the next section, we shall come to appreciate that a number of features of the spectrum are in fact weakly affected by the orientational order near the interface.

When the $Q_0 = 0$, the equation satisfied by the Green's function becomes simply

$$(A - i\omega\nu)G(z, z') - D \frac{\partial^2 G}{\partial z^2} = \delta(z - z'), \quad (4.1)$$

and it is an elementary matter to solve this equation. We phrase the result in language similar to that used in the next section's discussion. We introduce two functions $\psi^>(z)$ and $\psi^<(z)$ which are linearly independent solutions of the homogeneous version of Eq. (4.1). These functions are constructed to obey the boundary conditions

$$\lim_{z \rightarrow \infty} \psi^>(z) = 0, \quad (4.2a)$$

$$\lim_{z \rightarrow 0} \psi^<(z) = 0. \quad (4.2b)$$

We have the explicit forms

$$\psi^>(z) = e^{-kz}, \quad (4.3a)$$

$$\psi^<(z) = \sinh(kz), \quad (4.3b)$$

where

$$k = \left[\frac{A - i\omega\nu}{D} \right]^{1/2}, \quad \text{Re}k > 0. \quad (4.3c)$$

The Green's function may then be written¹⁷

$$G(z, z') = \frac{1}{DW} [\psi^>(z)\psi^<(z')\Theta(z' - z) + \psi^<(z)\psi^>(z')\Theta(z - z')], \quad (4.4)$$

$$\mathcal{S}(\omega) = \frac{k_B T}{Dk\omega} \left[\int_0^\infty dz e^{-(\gamma+k)z} \int_0^z dz' e^{-\gamma z'} \sinh(kz') + \int_0^\infty dz e^{-\gamma z} \sinh(kz) \int_z^\infty dz' e^{-(\gamma+k)z'} \right] \quad (4.6)$$

and after integration, we obtain the very simple expression

$$\mathcal{S}(\omega) = \frac{k_B T}{2\gamma D\omega} \frac{1}{(\gamma + k)^2}. \quad (4.7)$$

The imaginary part may be arranged to read

$$S(\omega) = \frac{k_B T}{2\gamma\omega} \frac{a(\omega)}{a^2(\omega) + b^2(\omega)}, \quad (4.8)$$

where

$$a(\omega) = \omega\nu + \gamma\sqrt{2D} [(A^2 + \omega^2\nu^2)^{1/2} - A]^{1/2} \quad (4.9a)$$

and

$$b(\omega) = D\gamma^2 + A + \gamma\sqrt{2D} [(A^2 + \omega^2\nu^2)^{1/2} + A]^{1/2}. \quad (4.9b)$$

There are several special limits of the above expressions worthy of attention. We consider them in sequence.

(1) $\omega\nu \ll A$ (low-frequency limit; $\gamma\xi$ general). Here one has

$$a(\omega) \cong \omega\nu(1 + \gamma\xi) \quad (4.10a)$$

and

$$b(\omega) \cong A(1 + \gamma\xi)^2 \gg a(\omega), \quad (4.10b)$$

where $\xi = (D/A)^{1/2}$ is the coherence length introduced earlier, in Sec. III. Thus we have

$$S(\omega) = \frac{k_B T}{2\gamma(1 + \gamma\xi)^3} \frac{\nu}{A^2} (\omega\nu \ll A). \quad (4.11)$$

We find a finite limit as $\omega \rightarrow 0$ for $S(\omega)$ by virtue of the restoring force for orientational fluctuations provided by the constraint A .

Now consider two opposite limiting cases.

(2) $A \gg D\gamma^2$ (equivalent to $\gamma\xi \ll 1$). To good approximation, we may set $D \equiv 0$ in the forms for $a(\omega)$

where W is the Wronskian of $\psi^>$ and $\psi^<$:

$$W = \psi^< \frac{\partial \psi^<}{\partial z} - \psi^> \frac{\partial \psi^>}{\partial z} \equiv k. \quad (4.5)$$

As expected, the Wronskian is independent of z .¹⁷ According to Eq. (3.11), the quantity of central interest is then

and $b(\omega)$. Then

$$S(\omega) \cong \frac{k_B T}{2\gamma} \frac{\nu}{A^2 + (\omega\nu)^2}, \quad (4.12)$$

and the light scattering spectrum is a Lorentzian central peak, with width controlled entirely by A . In this limit where $\gamma \rightarrow 0$, the light penetrates deeply in the liquid and the spectrum is reduced to the bulk expression of the scattering of the light by bulk liquid crystals.¹¹ In particular, we find the expression of de Gennes¹¹ for the relaxation time τ defined by the linewidth of the Lorentzian $\tau(T)^{-1} = \Gamma_0 = A(T)/\nu$.

(3) $D\gamma^2 \gg A$ (equivalent to $\gamma\xi \gg 1$). Here the penetration depth of the light is very small compared to the coherence length. One has

$$a(\omega) = (\omega\nu)^{1/2} [(\omega\nu)^{1/2} + (2D\gamma^2)^{1/2}] \quad (4.13a)$$

and

$$b(\omega) = (D\gamma^2)^{1/2} [(D\gamma^2)^{1/2} + (2\omega\nu)^{1/2}]. \quad (4.13b)$$

There are two special cases here:

(a) $\omega\nu \ll D\gamma^2$,

$$S(\omega) \cong \frac{k_B T}{\sqrt{2}D^{3/2}\gamma^4} \left[\frac{\nu}{\omega} \right]^{1/2} (A \ll \omega\nu \ll D\gamma^2). \quad (4.14a)$$

(b) $\omega\nu \gg D\gamma^2$, where again a simple limiting form applies,

$$S(\omega) \cong \frac{k_B T}{2\gamma\nu} \frac{1}{\omega^2} (A \ll D\gamma^2 \ll \omega\nu), \quad (4.14b)$$

which is the bulk expression [see Eq. (4.12)].

We now turn to a discussion of the significance of the above results. In the limit $A \ll D\gamma^2$, we then have the following picture of the spectrum. As the frequency approaches zero, $S(\omega)$ approaches the finite limit given in Eq. (4.11). Then when $\omega\nu \gg A$, but is small compared to $D\gamma^2$, Eq. (4.14a) applies. Evidently we have a central peak, which is flanked

by a very broad, slowly varying wing, which falls off as $\omega^{-1/2}$. Then finally, at large enough frequencies, when $\omega\nu$ exceeds $D\gamma^2$, the $\omega^{-1/2}$ behavior rolls over the ω^{-2} ; the crossover from the $\omega^{-1/2}$ to ω^{-2} behavior insures that $\int_0^\infty d\omega S(\omega)$ is finite.

It is now useful to examine some parameters characteristic of the liquid crystal MBBA. All of the parameters which enter our model have been deduced from light scattering studies of the bulk liquid.¹⁵ Recall that $A = a_L(T - T^*)$, and we have $a_L = 6.27 \times 10^{-2} \text{ J cm}^{-3} \text{ K}^{-1}$, with $T^* = 314 \text{ K}$. Then $B = 0.47 \text{ J cm}^{-3}$, $C = 0.79 \text{ J cm}^{-3}$, and $D = 4.43 \times 10^{-13} \text{ J cm}^{-1}$. These numbers imply $T_c = 315 \text{ K}$. The friction coefficient ν has a temperature dependence of the activated form, $\nu = \nu_0 \exp(2800/T)$, with $\nu_0 = 1.76 \times 10^{-11} \text{ J cm}^{-3} \text{ sec}$, so when $T = 315 \text{ K}$ we have $\nu \cong 1.3 \times 10^{-7} \text{ J cm}^{-3} \text{ sec}$ near 315 K . Finally, for scattering geometries such as those discussed earlier in the paper, Stegeman⁵ estimates that $\gamma \cong 5 \times 10^5 \text{ cm}^{-1}$.

These numbers give $D\gamma^2/A \sim 2$ near the phase transition when $T \cong T_c$. Thus the discussion of the limit $D\gamma^2 \gg A$ provides a qualitative picture of the nature of the spectrum, though $D\gamma^2$ is not so large for this limit to be fully appropriate. Note that, again near $T \cong T_c$, we have $A/2\pi\nu \cong 10^5 \text{ Hz}$. Frequency shifts the order of A/ν are thus too small to be accessible by Brillouin spectroscopy, and beating spectroscopy will be required for full access to the central region of the spectrum. Of course, the integrated strength of the central peak is measured much more easily, and this quantity contains valuable information also.

We shall see that the temperature dependence of the integrated central peak, $\int_0^\infty d\omega S(\omega)$, is a quantity of considerable interest. We would like to see the temperature dependence of this quantity explored in the reflection geometry, and compared to its bulk behavior. One may infer the behavior of this quantity from data on the total amount of light scattered diffusely from the surface, without the need for obtaining the complete frequency spectrum. We comment on this further, when the results of our full calculations are presented in Sec. VI.

At the end of Sec. III, we remarked that to good approximation, one may ignore the variation of the scattering cross section with \vec{q}_\parallel , the wave-vector change of the photon, projected onto the plane parallel to the interface. The influence of \vec{q}_\parallel on the spectrum follows if in Eq. (3.6) we replace $\partial^2/\partial z^2$ by the full Laplacian ∇^2 . Then all of the analysis above goes through unchanged, except A is replaced everywhere by the combination $A + Dq_\parallel^2$. Typical values of q_\parallel are $q_\parallel \cong 10^5 \text{ cm}^{-1}$, since q_\parallel^{-1} has the order of magnitude of the wavelength of the light

$T \cong T_c$, the ratio Dq_\parallel^2/A is the order of 0.1. Thus for the particular example that is the primary focus of the present paper, to good approximation we may set $\vec{q}_\parallel = 0$. Note that the expression $Dq_\parallel^2 \ll A$ can be read $\xi q_\parallel \ll 1$, which means that ξ is too small to induce a significant amount of correlation of motion between molecules separated by the distance of interest q_\parallel^{-1} in the xy plane. We then meet again the fact that correlations can be neglected in the xy plane.

The special limits explored in this section bear a close relationship to earlier work of Oliveros and Tilley.¹⁸ These authors consider the backscattering of light from entropy fluctuations near a surface. The basic equation they study is thus a diffusion equation, and in fact when we set $A = 0$ (and also $Q_0 = 0$ as everywhere in this section), then our theory is based on a simple diffusion equation also. Oliveros and Tilley obtain an $\omega^{-1/2}$ behavior of the cross section, and in their case the divergence extends right down to zero frequency. This $\omega^{-1/2}$ behavior is characteristic of scattering from two-dimensional fluctuations. The condition $\nu\omega \ll D\gamma^2$ which delineates the $\omega^{-1/2}$ regime means that the diffusion length $(D/\nu\omega)^{1/2}$ of fluctuations of frequency ω is very large compared with the penetration depth of optical fields into the liquid, so the fluctuations appear two dimensional to the light. When $\nu\omega \gg D\gamma^2$, the converse is true, and the fluid appears as a thin layer (effective thickness γ^{-1}) of three-dimensional fluid. Equation (4.19b) just describes the high-frequency tail of a diffusive central peak in a three-dimensional fluid. The scattering efficiency is proportional to γ^{-1} , as the above considerations require.

The other crossover, between the ω -independent and the $\omega^{-1/2}$ behavior of the spectra outlined by Eqs. (4.11) and (4.14a), takes place at $\omega \sim A/\nu$. We have already mentioned that this frequency is the inverse of the relaxation time for long-wavelength fluctuations in the bulk liquid crystal. However, when $\omega \gg A/\nu$, the relaxation of spatially nonuniform orientational fluctuations is controlled by diffusion rather than local restoring forces, and one then finds the $\omega^{-1/2}$ behavior discussed above. In Fig. 3, we present calculations of $S(\omega)$ for the model of MBBA described here, with $Q_0 = 0$. This crossover is illustrated in Fig. 3(a).

It follows from the above discussion that the part of the spectra $\omega \gg A/\nu$ is insensitive to the orientational order induced by the boundary. From a mathematical point of view, this results from the fact that the parameter A has dropped out in Eqs. (4.14). Then in what follows, we shall only focus our attention to the lower-frequency part of the spectra, typically $\omega < 10^7 \text{ sec}^{-1}$

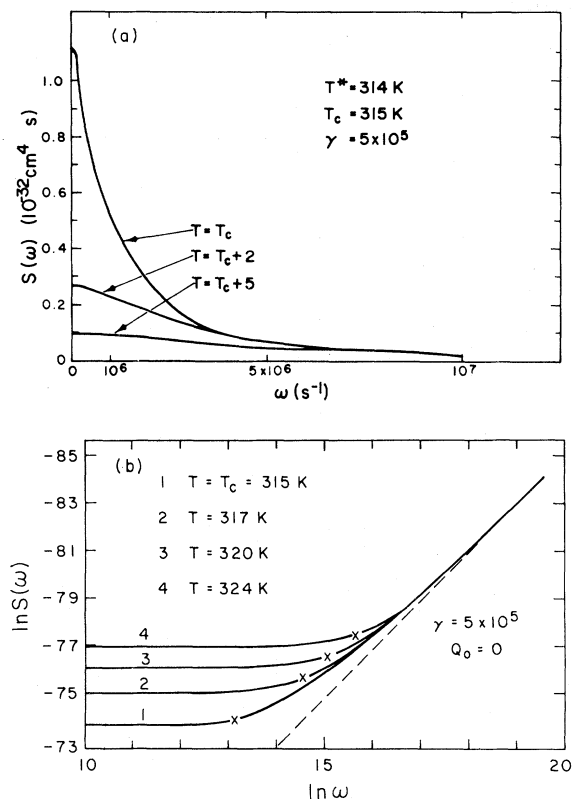


FIG. 3. For the case where $Q_0=0$, we plot (a) the function $S(\omega)$ defined in Eq. (4.8), and (b) the Neperian logarithm of $S(\omega)$. This is done for parameters characteristic of MBBA. The dashed line in (b) is the behavior expected from the $\omega^{-1/2}$ law in Eq. (4.14a). Crosses indicate the points of the curves where $\omega = A(T)/\nu$.

We are now ready to consider the general case with $Q_0 \neq 0$. Since this study leads us into rather complex algebraic formulas, the present section should provide orientation on the key features of the phenomena.

V. THE SOLUTION FOR GENERAL Q_0

We now turn to the general solution of Eq. (3.9), for $Q_0 \neq 0$. We shall see that it is possible to obtain a closed-form expression for the integral in Eq. (2.22), which is in the central expression in the theory. While we cannot express the integral in terms of elementary functions, nonetheless the final form is suitable for evaluation on a computer, with a modest expenditure of computer time. We remark that this section is devoted principally to an exposition of the mathematics of the full solution to the problem. The reader not interested in the rather complex formulas presented here may wish to

proceed directly to Sec. VI, where we present the results of our numerical calculations, and discuss the physical reasons for the trends evident in them.

We first consider the case $\omega \neq 0$, and we begin with the change of variables

$$y = 2d \exp(-z/\xi), \quad (5.1a)$$

$$W = \left[\frac{y}{2d} \right]^{1/2} G(z, z'; \omega), \quad (5.1b)$$

where in these expressions

$$d = Q_0 \xi \left[\frac{3C}{D} \right]^{1/2}. \quad (5.2)$$

With this change of variables,

$$\delta(z - z') = \left| \frac{dy}{dz} \right| \delta(y - y') = \frac{y}{\xi} \delta(y - y'), \quad (5.3)$$

so that Eq. (3.9) becomes, with $A' = A - i\omega\nu$,

$$\frac{d^2 W}{dy^2} + \left[\left(\frac{1}{4} - \frac{A' \xi^2}{D} \right) \frac{1}{y^2} + \frac{B \xi}{\sqrt{3CD}} \frac{1}{y} - \frac{1}{4} \right] W = \frac{\xi}{Dy} \left[\frac{y}{2d} \right]^{1/2} \delta(y - y'). \quad (5.4)$$

Upon defining a new function $H(y, y'; \omega)$

$$\begin{aligned} H(y, y'; \omega) &= - \frac{D(2dy')^{1/2}}{\xi} W(y, y'; \omega) \\ &= - \frac{D(yy')^{1/2}}{\xi} G(z, z'; \omega), \end{aligned} \quad (5.5)$$

and then interchanging y and y' on the right-hand side of Eq. (5.4) one has

$$\frac{d^2 H}{dy^2} + \left[\left(\frac{1}{4} - \frac{\xi^2 A'}{D} \right) \frac{1}{y^2} + \frac{B \xi}{(3CD)^{1/2}} \frac{1}{y} - \frac{1}{4} \right] H = \delta(y - y'). \quad (5.6)$$

The homogeneous version of Eq. (5.6) is in fact Whittaker's standard form of the confluent hypergeometric differential equation.¹⁹ There are two linearly independent solutions, written as¹⁹

$$M(y) = y^{c/2} e^{-y/2} \Phi(a, c; y) \quad (5.7a)$$

and

$$N(y) = y^{c/2} e^{-y/2} \Psi(a, c; y). \quad (5.6b)$$

Here the parameters a and c are given by

$$c = 1 + 2\xi \left[\frac{A - i\omega\nu}{D} \right]^{1/2} \quad (5.8a)$$

and

$$a = \frac{1}{2}c - \frac{B\xi}{(3CD)^{1/2}}, \quad (5.8b)$$

while $\Phi(a, c; y)$ is Kummer's hypergeometric series

$$\Phi(a, c; y) = \sum_{n=0}^{\infty} \frac{\Gamma(a)}{\Gamma(a+n)} \frac{\Gamma(c+n)}{\Gamma(c)} \frac{y^n}{n!}, \quad (5.9)$$

with Γ the usual gamma function. While $\Psi(a, c; y)$ is chosen so $N(y)$ and $M(y)$ are linearly independent, this condition alone does not specify $\Psi(a, c; y)$ uniquely. In Appendix A, we show that stability criteria applied to the thermodynamic fluctuations

$$H(y, y'; \omega) = -\frac{1}{W(M, N)} [M(y)N(y')\Theta(y-y') + M(y')N(y)\Theta(y'-y) + \alpha(y')M(y) + \beta(y')N(y)], \quad (5.11)$$

where $\Theta(x)$ is the Heaviside step function, which is equal to unity for positive values of its argument, and which vanishes for negative values. We have for the Wronskian $W = M dN/dy - N dM/dy$, a quantity independent of y ,¹⁷

$$W(M, N) = -\frac{\Gamma(c)}{\Gamma(a)}. \quad (5.12)$$

Equation (5.12) may be obtained from the behavior of M and N near $y=0$. The two functions $\alpha(y')$ and $\beta(y')$ are determined by requiring the Green's function to obey the boundary conditions, which in terms of the coordinate y read

$$\lim_{y \text{ or } y' \rightarrow 0} G = 0 \quad (5.13a)$$

and

$$\lim_{y \text{ or } y' \rightarrow 2d} G = 0. \quad (5.13b)$$

It follows that the full expression for the Green's function is then

$$G(z; z'; \omega) = -\frac{\Gamma(a)}{\Gamma(c)} \frac{\xi}{D} (yy')^{(c-1)/2} e^{-(1/2)(y+y')} \left[\Phi(y)\Psi(y')\Theta(y-y') + \Phi(y')\Psi(y)\Theta(y'-y) - \Psi(y')\Phi(y) - \Phi(y')\Psi(y) + \frac{\Psi(2d)}{\Phi(2d)}\Phi(y)\Phi(y') \right], \quad (5.14)$$

where for simplicity we drop explicit reference to the parameters a and c in Φ and Ψ .

Now we must turn our attention to the integration on z and z' in the expression for the light scattering cross section. While these integrals may be evaluated by numerical methods through resort to Eq. (5.14), it also turns out that one may obtain closed-form expressions for these objects, as remarked earlier. After some algebra, one may show that

$$\mathcal{S}(\omega) = \frac{\Gamma(a)}{\Gamma(c)} \frac{\xi^3 k_B T}{D\omega} \frac{1}{(2d)^{2\gamma\xi}} \left[\frac{\Psi(2d)}{\Phi(2d)} \left[\int_0^y dy y^{[\gamma\xi+(c-3)/2]} e^{-y/2} \Phi(y) \right]^2 - 2 \int_0^{2d} dy y^{[\gamma\xi+(c-3)/2]} e^{-y/2} \Psi(y) \int_0^y dy' y'^{[\gamma\xi+(c-3)/2]} e^{-y'/2} \Phi(y') \right]. \quad (5.15)$$

The explicit evaluation of the integral in Eq. (5.15) is reported in Appendix B. Here we only quote the result:

imply that $\Psi(a, c; y)$ is the function defined by Tricomi.²⁰ If c is not an integer (i.e., if $\omega \neq 0$), the $\Psi(a, c; y)$ is given by

$$\Psi(a, c; y) = \frac{\Gamma(1-c)}{\Gamma(a-c+1)} \Phi(a, c; y) + \frac{\Gamma(c-1)}{\Gamma(a)} y^{1-c} \Phi(a-c+1, 2-c; y). \quad (5.10)$$

Then the Green's function which satisfies the boundary conditions stated in Eq. (3.11) has the form¹⁷

$$\begin{aligned}
 \mathcal{S}(\omega) = & \frac{\xi^3 k_B T}{D\omega} \frac{\Gamma(c)}{\Gamma(a)} (2d)^{c-3} e^{-2d} \\
 & \times \left\{ \frac{\Psi(a, c; 2d)}{\Phi(a, c; 2d)} (2d)^2 \left[\sum_{n=0}^{\infty} \frac{\Gamma(a+n)}{n! \Gamma(c+n)} (2d)^n \frac{\Phi(1, \gamma\xi + (c-3)/2 + n + 2, d)}{\gamma\xi + (c-3)/2 + n + 1} \right]^2 \right. \\
 & - 2(2d)^{3-c} \sum_{n=0}^{\infty} \frac{\Gamma(a+n)}{n! \Gamma(c+n)} \Gamma(\gamma\xi + (c-3)/2 + n + 1) (2d)^n \\
 & \times \sum_{m=0}^{\infty} \frac{d^m}{\Gamma(\gamma\xi + (c-3)/2 + n + m + 2)} \\
 & \times \left[\frac{1}{c-1} \left[\frac{\Phi(1, 2\gamma\xi + n + m + 1; 2d)}{2\gamma\xi + n + m} \right. \right. \\
 & \left. \left. + \frac{(a-c+1)}{(2-c)} \frac{2d\Phi(1, 2\gamma\xi + n + m + 2; 2d)}{2\gamma\xi + n + m + 1} \right] \right. \\
 & + \frac{(2d)^2 \Gamma(1-c)}{\Gamma(a-c+1)} \\
 & \times \sum_{p=0}^{\infty} \frac{(2d)^p}{p!} \left[\frac{\Gamma(a+p)}{\Gamma(c+p)} \frac{\Phi(1, 2\gamma\xi + n + m + p + c; 2d)}{2\gamma\xi + n + m + p + c - 1} (2d)^{c-3} \right. \\
 & \left. - \frac{\Gamma(a-c+3+p)}{\Gamma(4-c+p)(p+1)(p+2)} \right. \\
 & \left. \left. \times \frac{\Phi(1, 2\gamma\xi + n + m + p + 3; 2d)}{2\gamma\xi + n + m + p + 2} \right] \right\} \quad (5.16)
 \end{aligned}$$

We now turn to the calculation of the Green's function for the limit $\omega=0$. As remarked earlier, in this case, c becomes the integer 3 and the Ψ function acquires a logarithmic singularity. The case $\omega=0$ is of considerable interest, because it is correlated to the integrated strength of the central peak. In effect the Kubo's theorem derived in Eq. (A3) leads to

$$S_E = \frac{1}{\pi} \int_{-\infty}^{+\infty} \text{Im} \mathcal{S}(\omega) d\omega = \lim_{\omega \rightarrow 0} \omega \text{Re} \mathcal{S}(\omega) \quad (5.17)$$

since $\mathcal{S}(\omega)$ is proportional to $G(z, z'; \omega)/\omega$. The quantity S_E defined in Eq. (5.17) is directly proportional to the scattering efficiency per solid angle, $\int \mathcal{E}(\omega) d\omega$, where $\mathcal{E}(\omega)$ has been defined in Eq. (2.18). To calculate this expression, we can generate the Tricomi function for $c=3$ from its general integral representation, and we use this result to recalculate $\text{Re} \mathcal{S}$ when $\omega \rightarrow 0$. This is done in Appendix B. We may arrive at the same result by directly taking the limit of Eq. (5.16) when $c \rightarrow 3$. We let $c=3+\epsilon$ and take the limit of various singular quantities as $\epsilon \rightarrow 0$, by the use of their Taylor's expansion as a function of ϵ . We can write

$$\begin{aligned}
 (2d)^\epsilon &= 1 + \epsilon \ln 2d + \dots, \\
 \frac{d}{dc} \frac{1}{\Gamma(c+p)} &= - \frac{1}{\Gamma(c+p)} \tilde{\psi}(\frac{1}{2} + c), \quad (5.18a)
 \end{aligned}$$

and from Eq. (B16),

$$\frac{d}{dc} \left[\frac{e^{-2d} \Phi(1, a+c; 2d)}{\alpha+c-1} \right] = - \sum_{n=1}^{\infty} \frac{(-1)^n (2d)^n}{n! (\alpha+c+n-1)^2}, \quad (5.18b)$$

where $\tilde{\psi}$ is the logarithmic derivation of the gamma function, or the digamma function. Equation (5.18a) is

used to take the limit of various quantities appearing in Eq. (5.10), to derive the expression of the Tricomi function

$$\Psi(a;3;2d) = \frac{(2d)^{-2}}{\Gamma(a)} + \frac{(2-a)}{\Gamma(a)}(2d)^{-1} \frac{1}{2\Gamma(a-2)} \Phi(a,3,2d) \ln 2d - \frac{1}{\Gamma(a)\Gamma(a-2)} \sum_{r=0}^{\infty} [\tilde{\psi}(a+r) - \tilde{\psi}(1+r) - \tilde{\psi}(3+r)] \frac{\Gamma(a+r)}{(r+2)!r!} (2d)^r. \tag{5.19}$$

Also, since $\Gamma(1-c) = \Gamma(4-c) / [(3-c)(2-c)(1-c)]$, we have

$$\lim_{\epsilon \rightarrow 0} \epsilon \Gamma(1-c) = -\frac{1}{2}. \tag{5.20}$$

Then Eqs. (5.18a), (5.18b), and (5.20) are used to evaluate the terms of the summation over p in Eq. (5.16), via l'Hospital's rule, to give

$$S_E = \frac{\xi^3 k_B T}{D} \frac{2e^{-2d}}{\Gamma(a)} \left\{ \frac{\Psi(a,3;2d)}{\Phi(a,3;2d)} (2d)^2 \left[\sum_{n=0}^{\infty} \frac{\Gamma(a+n)}{n!(n+2)!} \frac{(2d)^n \Phi(1, \gamma\xi + n + 2; d)}{\gamma\xi + n + 1} \right]^2 - \sum_{n=0}^{\infty} \frac{\Gamma(a+n)}{n!(n+2)!} \Gamma(\gamma\xi + n + 1) (2d)^n \right. \\ \times \sum_{m=0}^{\infty} \frac{(d)^m}{\Gamma(\gamma\xi + n + m + 2)} \\ \times \left[\frac{\Phi(1, 2\gamma\xi + n + m + 1; 2d)}{2\gamma\xi + n + m} + (2-a) \frac{2d \Phi(1, 2\gamma\xi + n + m + 2; 2d)}{2\gamma\xi + n + m + 1} \right. \\ \left. + \sum_{p=0}^{\infty} \frac{(2d)^2}{\Gamma(a-2)} \frac{\Gamma(a+p)}{\Gamma(3+p)} \frac{(2d)^p}{p!} \right. \\ \left. \times \left[\frac{\Phi(1, 2\gamma\xi + n + m + p + 3; 2d)}{2\gamma\xi + n + m + p + 2} \right. \right. \\ \left. \left. \times [\tilde{\psi}(3+p) + \tilde{\psi}(p+1) - \tilde{\psi}(a+p) - \ln(2d)] \right. \right. \\ \left. \left. + \sum_{q=0}^{\infty} \frac{(-1)^q e^{2d} (2d)^q}{q! (2\gamma\xi + n + m + p + q + 2)^2} \right] \right\}. \tag{5.21}$$

The limit of the imaginary part of $\mathcal{S}(\omega)$, when $\omega=0$, i.e., $S(0)$ is also a useful quantity, since it gives the amplitude of the central peak, at zero frequency drift. We can also derive the explicit expressions of $S(0)$ by analyzing the limit of $\mathcal{S}(\omega)$ when $\omega \rightarrow 0$, as in the derivation of S_E . The method, however, becomes clumsy, because $\text{Im}G(z, z'; \omega)$ vanishes as $\omega \rightarrow 0$, so that the series in Eq. (5.16) must be developed up to the first order in ω or in ϵ to evaluate the singular ratio $\text{Im}G(z, z'; \omega) / \omega$, although the zeroth-order terms were sufficient to evaluate S_E . So, the full expression of $S(0)$ is complex and we do not report it here. Moreover, it is easier to compute $S(0)$ directly from Eq. (5.16), because $S(\omega)$ tends to a constant at small value of ω , according to Eq. (4.11).

From the general expressions given in this section, we can also recover the simple results in Sec. IV, in which we have $Q_0=0$. For this purpose, we note from Eq. (5.2) that to achieve this limit, we want to let $d \rightarrow 0$ in the final expression given by Eq. (5.16). Thus all the Φ functions are replaced by unity, and from Eq. (5.10)

$$\lim_{d \rightarrow 0} \Psi(a; c; 2d) = \frac{\Gamma(c-1)}{\Gamma(a)} (2d)^{1-c}. \tag{5.22}$$

Then the only two terms in Eq. (5.16) which contribute are those with $n=m=0$, and all terms with index p vanish. It then follows that

$$\lim_{\omega \rightarrow 0} \mathcal{S}(\omega) = \frac{\xi^2 k_B T}{2D\gamma\omega} \frac{1}{[\gamma\xi + (c-3)/2 + 1]^2}, \tag{5.23}$$

a result quite identical to Eq. (4.8).

In Sec. VI, we use the general expressions in this section to examine the influence of orientational order on $S(\omega)$.

VI. RESULTS AND DISCUSSION WHEN $Q_0 \neq 0$

In Sec. IV, we discussed the nature of the light scattering spectrum when $Q_0 = 0$, and here we turn to the case where orientational order is present near the interface, so $Q_0 \neq 0$. All calculations are performed with the material MBBA in mind, and the parameters we have used are those quoted near the end of Sec. IV. The calculations are presented for various values of the temperature, and for the purpose of presentation, we suppose Q_0 is fixed independent of temperature. We have seen that Miyano's data is consistent with the model presented in Sec. III, which gives $Q_0 \sim (T - T_c)^{-1/2}$, but magnitude of the prefactor is not known, so we regard Q_0 as a parameter that may be varied independently of temperature. If the results presented here were to be compared with data, it would then be possible to obtain a second source of data with the temperature variation of Q_0 . As we have remarked earlier, estimates give $\gamma \cong 5 \times 10^5 \text{ cm}^{-1}$; we have allowed γ to vary between $2 \times 10^5 \text{ cm}^{-1}$ and 10^6 cm^{-1} in the calculations reported below, to illustrate the influence of variations in the optical penetration depth on the spectra.

We begin with a series of figures which show general trends in the calculated spectra. In Fig. 4, we plot $\ln S(\omega)$ against $\ln(\omega)$ for two values of Q_0 , for values of γ in the range outlined above and for the case where the temperature equals T_c . As γ increases, and the penetration depth of the light decreases, we expect $S(\omega)$ to decrease as illustrated, but in fact the decrease is much more dramatic than that caused by the decrease in scattering volume alone, proportional to γ^{-1} . The reason is that in this range of frequencies, the spectrum is proportional to this scattering volume only in the limit $\gamma\xi \ll 1$. This can readily be seen from Eq. (4.11). This condition is not fulfilled for the values of γ investigated, since $\gamma\xi \cong 1$. When $\gamma\xi \gg 1$, one has $S(\omega) \propto \gamma^{-4}$ at low frequencies, so the dramatic variation of $S(\omega)$ with γ in Fig. 4 is not surprising. At frequencies larger than those shown in the plot, $S(\omega)$ settles into the $\omega^{-1/2}$ behavior described in Sec. IV. In our case, this occurs well out in the wing of $S(\omega)$, where the scattering intensity is orders of magnitude smaller than in the central peak. For later purposes, notice that when $Q_0 = 1$, $S(\omega)$ has decreased, compared to the case $Q_0 = 0.6$.

Figure 5 shows the behavior of $S(\omega)$ as a function of temperature. In the region of the central peak

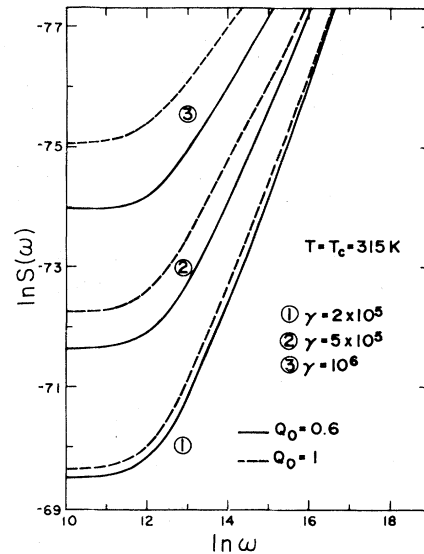


FIG. 4. When $T = T_c$, we give a Neperian logarithmic plot the spectral density function $S(\omega)$, as a function of frequency, for two values of the surface pinning parameter Q_0 , and attenuation constant γ of the light. Parameters appropriate to MBBA are employed. γ is expressed in cm^{-1} .

and with $Q_0 = 0.6$, the scattering intensity increases dramatically as T_c is approached from above, and the central peak narrows. It is useful to note that right at T_c , the correlation length is equal to 200 \AA

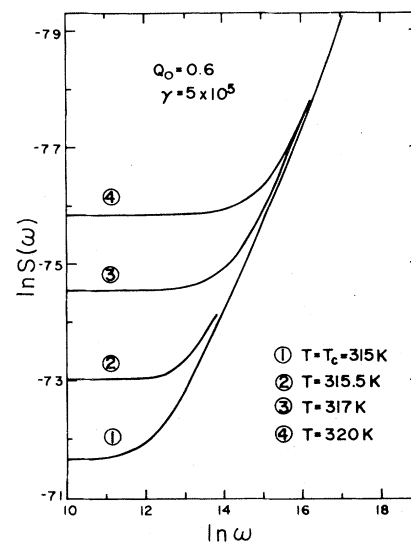


FIG. 5. For several temperatures near T_c , and $Q_0 = 0.6$, we show a Neperian logarithmic plot of $S(\omega)$ vs frequency. Parameters are those appropriate to MBBA with $\gamma = 5 \times 10^5 \text{ cm}^{-1}$. The plot shows the $\omega^{-1/2}$ behavior, at frequencies sufficiently high that the various curves have coalesced.

for our choice of parameters, so $\gamma\xi \cong 1$ right at T_c . Figure 5 extends far enough in frequency for the $\omega^{-1/2}$ behavior to become apparent in the wing of the central peak. This is the frequency regime where the various curves coalesce.

In Fig. 6, for $Q_0=0$ and $Q_0=0.6$, we compare the temperature variation of $S(\omega=0)$, which measures the intensity of the central peak at $\omega=0$. It is evident that the substrate induced orientational order can have a dramatic effect on the temperature variation of the total amount of light scattered diffusely from the substrate. It should not be too difficult to measure the integrated strength of the central peak of light back scattered from the interface, and compare its temperature dependence with that of the central peak in the bulk liquid. Such data would provide useful evidence for central peak anomalies in the back-scattering experiment of interest here, without the need of examining small frequency shifts the order of A/ν . It is perhaps surprising that by *pinning* the order parameter at the interface ($Q_0=0.6$ rather than $Q_0=0$), one *enhances* the intensity of the central peak, i.e., one enhances the amplitude of the order-parameter fluctuations near the boundary. We shall appreciate the reasons for this shortly.

When Q_0 is increased from 0 to 1, at T_c , the in-

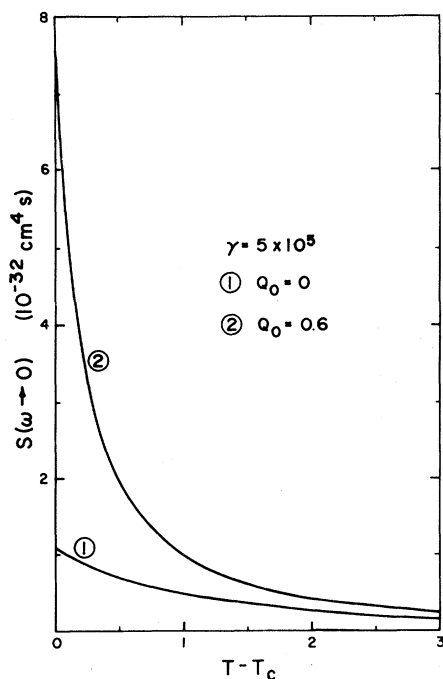


FIG. 6. Plot of $S(\omega=0)$ vs $(T-T_c)$ for two values of Q_0 . This function is the intensity of the central peak at $\omega=0$ in the light scattering spectrum. Parameters appropriate to MBBA have been used with $\gamma=5 \times 10^5 \text{ cm}^{-1}$.

tensity of the central peak at $\omega=0$ first increases, to reach a maximum when $Q_0 \cong 0.6$, then decrease as Q_0 is increased to unity. In Figs. 7(a) and 7(b), on logarithmic and linear plots, respectively, we show the dependence of the central peak intensity at $\omega=0$ on Q_0 , for $0 \leq Q_0 \leq 0.6$. It is evident from Fig. 4, as remarked earlier, that for the parameters we use, the intensity of the central peak first grows with Q_0 , then decreases.

The effect of Q_0 on the temperature variation of $S(\omega)$ is most pronounced very near the critical temperature. This is illustrated in Fig. 8, where for

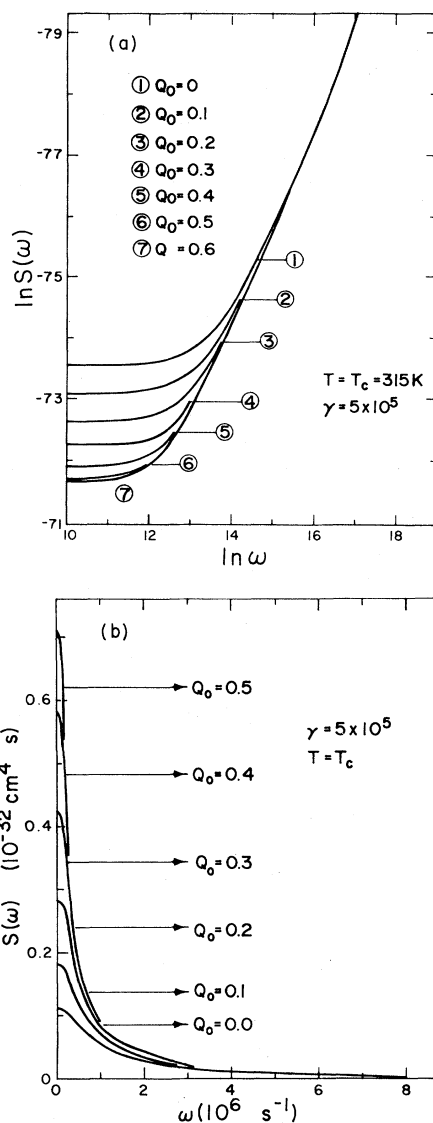


FIG. 7. For several values of Q_0 in the range $0 < Q_0 \leq 0.6$, we plot the frequency variation of $S(\omega)$. We give (a) a Neperian logarithmic plot, and (b) a direct plot of $S(\omega)$, in the case $\gamma=5 \times 10^5 \text{ cm}^{-1}$.

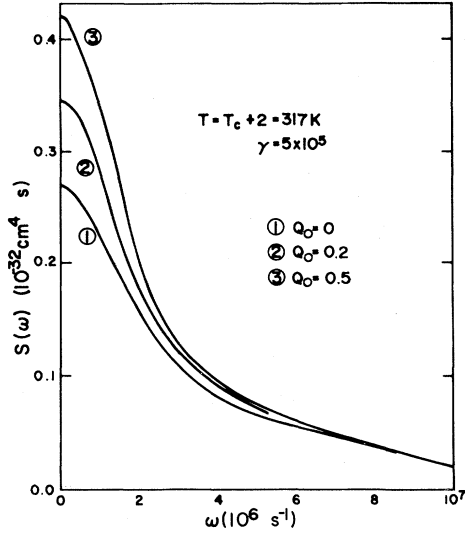


FIG. 8. Frequency variation of $S(\omega)$ for parameters relevant to MBBA, with $\gamma = 5 \times 10^5 \text{ cm}^{-1}$ and for several values of Q_0 , at a temperature somewhat above T_c .

three values of Q_0 , we plot the frequency variation of $S(\omega)$, at a temperature two degrees above T_c . There is quite clearly a variation with Q_0 , but it is modest in comparison to the calculations right at T_c .

We now pause to present a discussion which provides insight into the physical origin of the trends displayed in Fig. 4 through Fig. 7. The equation obeyed by the Green's function has the form

$$\nu \frac{\partial G}{\partial t} + V(z)G - D \frac{\partial^2 G}{\partial z^2} = \delta(z - z')\delta(t - t'). \quad (6.1)$$

The function $\Gamma_1(z) = V(z)/\nu$ may be viewed as a local relaxation frequency which varies from point to point near the surface, and the third term on the right-hand side allows the fluctuations to diffuse.

One may write

$$V(z) = V_0 + V_1(z), \quad (6.2)$$

where

$$V_0 = A(T - T^*) - \frac{1}{3} \frac{B^2}{C} \quad (6.3)$$

and

$$V_1(z) = \frac{B^2}{3C} \left[1 - \exp \left[-\frac{1}{\xi}(z - z_0) \right] \right]^2 \quad (6.4a)$$

$$\equiv V_1^{(\infty)} \left[1 - \exp \left[-\frac{1}{\xi}(z - z_0) \right] \right]^2, \quad (6.4b)$$

where

$$z_0 = \xi \ln \left[\frac{3CQ_0}{B} \right] \quad (6.5a)$$

and

$$V_1^{(\infty)} = \frac{B^2}{3C}. \quad (6.5b)$$

With the equation cast into this form, the homogeneous version of Eq. (6.1) is virtually identical to the Schrödinger equation of a particle with mass $\mu = \hbar/2D$ which moves in under the influence of the Morse potential²¹; the difference is that to generate Eq. (6.1), one must allow the time variable to become pure imaginary. We may use this analogy to obtain an alternate representation of the Green's functions. If $q_m(z)e^{-\lambda_m t}$ is the eigenfunction (chosen real) of the Morse potential problem just outlined and $\hbar\omega_m = \nu\lambda_m$ the eigenvalue, then we have

$$G(z, z'; \omega) = \frac{k_B T}{\nu} \sum_m \frac{q_m(z)q_m(z')}{\lambda_m - i\omega}. \quad (6.6)$$

The eigenvalue spectrum of the Morse potential is^{21,22}

$$\omega_n = \omega_e \left(n + \frac{1}{2} \right) \left[1 - \lambda \left(n + \frac{1}{2} \right) \right], \quad (6.7)$$

where, in terms of our parameters

$$\hbar\omega_e = \frac{\hbar}{\xi} \left[\frac{2V_1^{(\infty)}}{\mu} \right]^{1/2} = \frac{2}{\xi} \left[\frac{DB^2}{3C} \right]^{1/2} \quad (6.8)$$

and

$$\lambda = \frac{\hbar\omega_e}{4V_1^{(\infty)}} = \left[\frac{A(T)}{6A(T_c)} \right]^{1/2}, \quad (6.9)$$

where $A(T_c) = 2B^2/9C$ is the value of the parameter $A(T) = a_L(T - T^*)$ which enters the Landau-Ginsburg free-energy functional, evaluated at the temperature $T = T_c$.

Quite clearly, at $T = T_c$, $\lambda = 1/\sqrt{6}$, and under these conditions the Morse potential admits only a single bound state. The maximum quantum number n_M for which the eigenstate is bound²¹ is the first integer smaller than $(1 - \lambda)/2\lambda$, and in our case the inequality is satisfied only by $n = 0$. Under circumstances which will be detailed below, it is this single bound state which dominates the Green's function in Eq. (6.6) at low frequency, since λ_0 is the lowest value of the λ_m in the denominator of the series terms. Thus, upon form $S(\omega)$, we have

$$S(\omega) = \frac{k_B T}{\omega} \int_0^\infty dz \int_0^\infty dz' \text{Im}[G(z, z'; \omega)] e^{-\gamma(z+z')} \quad (6.10a)$$

$$= \frac{k_B T}{\nu} \frac{1}{\omega^2 + \lambda_0^2} \left[\int_0^\infty dz e^{-\gamma z} q_0(z) \right]^2 \quad (6.10b)$$

and the frequency λ_0 is given by $\nu\lambda_0 = V_0 + \hbar\omega_0$ which may be written

$$\nu\lambda_0 = A(T) - \left[\left(\frac{B^2}{3C} \right)^{1/2} - \frac{1}{2} [A(T)]^{1/2} \right]^2. \quad (6.11)$$

It is clear that λ_0 is *lower* than the characteristic fluctuation frequency of the bulk liquid. In fact, we must have $\lambda_0 > 0$ for stability of the system, and after some algebra one may show that this requires $A(T)/A(T_c) > \frac{2}{3}$, a condition that is obviously satisfied for all temperatures T greater than T_c . As expected from Appendix B, our system is always dynamically stable.

The reason why λ_0 is less than $A(T)/\nu$ may be appreciated by examining the variation with z of the local relaxation frequency $\Gamma_l(z)$. There are two possible behaviors. Let Q_0 sufficiently large that $Q_0 > B/3C$, so z_0 in Eq. (6.5a) is positive. Then as the point z moves from the bulk liquid toward the interface, $\Gamma_l(z)$ *decreases*, to pass through a minimum at z_0 ; at the minimum, $\Gamma_l(z_0) < \Gamma_l(\infty)$, so there is a region around the minimum where the local fluctuation frequency is *lower* than that in the bulk liquid. In the near vicinity of z_0 , the amplitude of the fluctuation is then necessarily *larger* than in the bulk. This can be regarded as a direct consequence of a Heisenberg principle which applies due to the analogy between Eq. (6.1) and a Schrödinger equation. If $Q_0 < B/3C$, the minimum in $\Gamma_l(z)$ is at the interface $z=0$. We conclude that pinning the order parameter at the interface necessarily always produces a local region near the interface where $\Gamma_l(z) < \Gamma_l(\infty)$. Thus we have a region of enhanced fluctuations near the interface, and at the same time a narrowing of the central peak.

The behavior outlined in the previous paragraph requires $B \neq 0$, i.e., we obtain a lowering of $\Gamma_l(z)$ near the interface *only* when the phase transition is first order. With $B \equiv 0$, $\Gamma_l(z) = A(T) + 3Q_0^2 \times \exp(-2z/\xi)$, and $\Gamma_l(z)$ is a monotonically decreasing function of z , so here pinning of the order parameter can only stiffen the response of the system near the interface. Thus had we applied our model to a magnetic surface or interface, where time-reversal symmetry requires $B \equiv 0$, then we would have found qualitatively different behavior.

We next examine the conditions under which the region of enhanced fluctuation dominates the light scattering spectrum, i.e., the conditions under which the matrix element in Eq. (6.10b) is sufficiently large

for the bound state eigenvalue to dominate the low-frequency behavior of the Green's function. If $Q_0 \gg B/3C$, we shall find $z_0 \gg \xi$, and we have seen $\xi\gamma \sim 1$. For very large Q_0 , the regime of enhanced fluctuations lies too far into the fluid for them to be probed by the light. Thus if we begin with very large Q_0 , and decrease this parameter, z_0 moves toward the interface, and when $z_0\gamma \sim 1$, the regime of enhanced fluctuation contributes strongly to the spectrum. For small Q_0 , the minimum in $\Gamma_l(z)$ is at $z=0$ since $z_0 < 0$, but is a very shallow feature which extends far into the fluid. The bound state is now very spread out, with little integrated strength inside the optical penetration depth, and does not dominate the behavior of $S(\omega)$. Thus we expect as Q_0 is increased for the central peak to increase in strength and narrow down, when compared to the bulk, but then for large Q_0 the regime of enhanced fluctuation is pushed too far into the fluid for the light to probe it, and the intensity of the narrow feature in $S(\omega)$ drops off. This is precisely the behavior we find in Fig. 9 through Fig. 7. If we argue that the maximum occurs when $z_0 = \gamma^{-1} \simeq \xi$ (for $\gamma \simeq 5 \times 10^5 \text{ cm}^{-1}$), then Eq. (6.5a) predicts the maximum in the central peak will occur at $Q_0 \simeq 0.59$, remarkably close to the results of the full calculations.

We now present results which show how the above picture may be used to fit systematic trends in the calculations. Figure 9 shows the variation of $S(\omega=0)$, the strength of the central peak at $\omega=0$, with Q_0 when $T=T_c$. The maximum referred to in each curve is clearly evident, and occurs when γz_0 is of order unity, as the preceding paragraph suggests. In Fig. 10, we illustrate the effects for three different temperatures near T_c .

In Fig. 11, we show the full width at half maximum of the central peak, normalized to the value $\Gamma_0 = A/\nu$ characteristic of the bulk liquid. The dashed line is the value λ_0 predicted from Eq. (6.11), and we see that for $Q_0 \geq 0.5$, where the minimum z_0 in $\Gamma_l(z)$ is well away from the interface, Eq. (6.11) accounts nicely for the width calculated from the full expression. When $Q_0 \geq 0.5$, the central peak in the back-scattering geometry is fitted rather well by the Lorentzian form in Eq. (4.12), with A/ν replaced by the appropriate reduced relaxation frequency λ_0 given in Eq. (6.11). For $Q_0 < 0.5$, we do not find the simple Lorentzian behavior, and for reasons outlined above, the low-frequency behavior of the Green's function is not dominated by the lowest eigenvalue, since the condition $Q_0 \gg B/(3C)$ is no longer fulfilled.

As we noted in Sec. I, the basic model explored here may serve as a suitable phenomenology not only for the description of orientational fluctuations in liquid crystals, but for order-parameter fluctua-

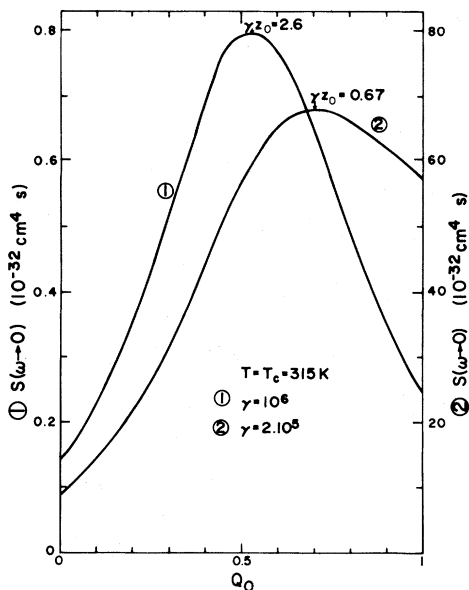


FIG. 9. For the two values of γ indicated in cm^{-1} , we plot the intensity of the central peak at zero frequency [$S(\omega=0)$] as a function of Q_0 , when the temperature T equals T_c . Note that a separate scale is used for each curve.

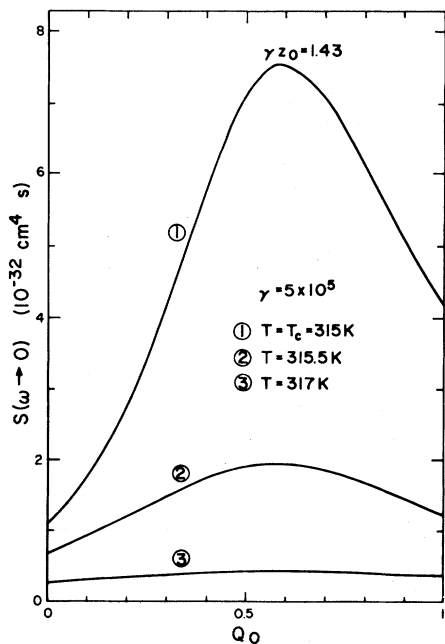


FIG. 10. For three different temperatures, and for $\gamma=5 \times 10^5 \text{ cm}^{-1}$, we show the variation of the strength of the central peak at zero frequency with the parameter Q_0 .

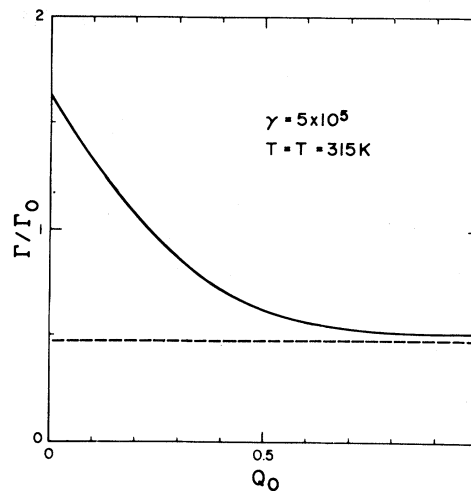


FIG. 11. Ratio Γ/Γ_0 as a function of Q_0 , when $T=T_c$, for $\gamma=5 \times 10^5 \text{ cm}^{-1}$. Here Γ_0 is the width of the central peak in the bulk liquid, and Γ is the width realized in the backscattering geometry. The dashed line is the value of the ratio predicted from Eq. (6.11).

tions near boundaries in other physical situations where a Landau-Ginzburg free-energy functional of similar form may be applied. Through use of the Morse-potential analogy, it may be possible to appreciate the key feature in the profile of order-parameter fluctuations without the need of evaluating the rather formidable series provided by the full theory.

The applicability of the model may also be extended to study very different surface problems. We briefly relate our results to those of a recent theory of the photocurrent conversion efficiency in a Schottky barrier, since a very similar mathematical analysis is encountered. Jarrett has solved the diffusion equation for the Schottky barrier illuminated with band-gap light,²³ using the Green's-function method. In that case the homogeneous part of the differential equation satisfied by the Green's function is Weber's equation instead of a confluent hypergeometric equation, but such equations only differ by a suitable change of variable. In particular the parabolic cylinder functions $E_{-\nu}^{(0)}(z)$ and $E_{-\nu}^{(1)}(z)$ which, by definition, are solutions of Weber's equation are also confluent hypergeometric functions²⁴:

$$E_{-\nu}^{(0)}(z) = 2^{1/2} e^{-z^2/4} \Phi \left[+\frac{\nu}{2}, \frac{1}{2}; \frac{z^2}{2} \right], \quad (6.12)$$

$$E_{-\nu}^{(1)}(z) = 2^{3/2} e^{-z^2/4} \Psi \left[+\frac{\nu}{2}, \frac{1}{2}; \frac{z^2}{2} \right].$$

In his paper, Jarrett has only studied the solutions

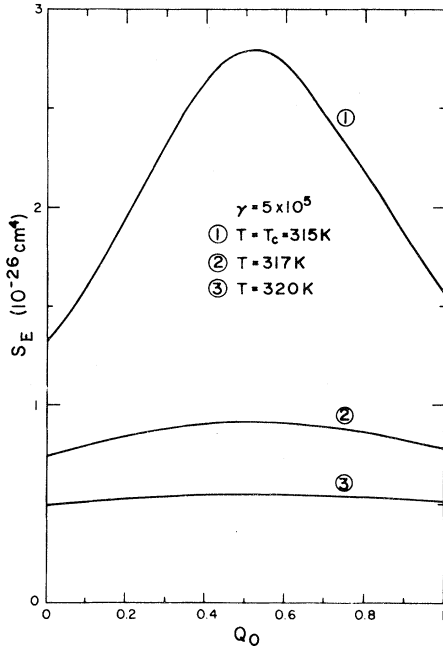


FIG. 12. Variation with Q_0 of the integrated strength of the central peak, S_E , as a function of Q_0 , for the temperatures near T_c , with $\gamma = 5 \times 10^5 \text{ cm}^{-1}$.

for special values of ν , namely ν equal to a positive integer $\nu = +n$ where these functions take simplified forms. If we refer to Eqs. (5.7), this condition could read $2a = +n$. In the same way, our numerical calculations are simplified in the particular case $a = -n$, which may happen when $\omega = 0$ according to Eq. (5.8). In that case, all the terms of the form $\Gamma(a+m)/\Gamma(a)$ entering Eq. (5.21) vanish for $m > n$, due to the divergence of $\Gamma(a)$ in the denominator. It follows that the series in Eq. (5.21) are reduced to polynomials of order n as a function of d . The reason is that $\Phi(a, c, x)$ and $\Psi(a, c, x)$ are reduced to Laguerre polynomials of order n , $L_n^{c-1}(x)$:

$$\begin{aligned} L_n^{c-1}(x) &= \frac{\Gamma(c+n)}{\Gamma(c)n!} \Phi(-n; c; x) \\ &= \frac{(-1)^n}{n!} \Psi(-n, c; x). \end{aligned} \quad (6.13)$$

If we refer to the analogy with the Morse potential in quantum mechanics, we can notice that such Laguerre polynomials give the radial part of the wave function,^{21,22} while the condition $a = -n$ is the equation which states the quantization of the levels $\hbar\omega_n$ defined in Eq. (6.8).²⁵ The advantage of the numerical procedure outlined in Appendix C is that it allowed us to obtain the solution of our problem for any value of the parameters entering the model, without the need to look at special limiting cases.

We conclude with Fig. 12 which shows the variation of the integrated strength S_E [Eq. (5.21)] of the cross section with Q_0 , for several values of the temperature near T_c . The variation of S_E is qualitatively similar to that of $S(\omega=0)$, though changes in the width of the central peak influence the variation of the integrated strength of the cross section. We find, for the parameters characteristic of MBBA, that $S_E \cong 10^{-26} \text{ cm}^4$. When this value is used in Eq. (2.18), we find the estimate of 10^{-8} for the integrated strength of the central peak per unit solid angle. We understand this value is sufficiently large that one should be able to detect the scattering.

ACKNOWLEDGMENTS

Both authors have enjoyed stimulating discussions with Professor G. Stegeman during the course of this investigation. This research has been supported in part by the U.S. Air Force Office of Scientific Research, under Contract No. F49620-C-0019.

APPENDIX A: STABILITY CRITERIA AND THE Ψ FUNCTION

Quite clearly, considerations of thermodynamics stability require that the function $\langle \delta Q(z, t) \delta Q(z', t) \rangle$ remain finite for all values of z and z' . From Eq. (2.14) we have

$$\langle \delta Q(z, t) \delta Q(z', t) \rangle = \int \frac{d\omega}{2\pi} \langle \delta Q(z) \delta Q(z') \rangle_{\omega}, \quad (A1)$$

which as we have seen may be written

$$\langle \delta Q(z; t) \delta Q(z', t) \rangle = \frac{k_B T}{\pi} \int \frac{d\omega}{\omega} \text{Im}[G(z, z'; \omega)] \quad (A2)$$

which, by virtue of the Kramers-Kronig relation which connects the real and imaginary part of the Green's function becomes

$$\langle \delta Q(z, t) \delta Q(z', t) \rangle = k_B T \text{Re}[G(z, z'; 0)]. \quad (A3)$$

Thus we require $G(z, z'; 0)$ to be finite. From Eq. (5.7), this requires $\lim_{\omega \rightarrow 0} \Psi$ be finite. When c is not an integer, the two solutions $\Phi(a, c; y) = y^{1-c} \Phi(a-c+1, 2-c; y)$ are linearly independent.²⁵ However, when $\omega \rightarrow 0, c$ as defined in Eq. (5.8) is an integer ($c=3$), and the second of these functions diverges for all y . According to Eq. (5.9), we may write

$$\begin{aligned} & \frac{y^{1-c}}{\Gamma(2-c)} \Phi(a-c+1, 2-c; y) \\ &= \sum_{n=0}^{\infty} \frac{\Gamma(a-c+1+n)}{\Gamma(a-c+1)} \frac{y^{n+1-c}}{\Gamma(2-c+n)} \frac{1}{n!}. \end{aligned} \quad (A4)$$

Consider the case where $c \rightarrow m + 1$, where m is an integer. Then $\Gamma(2 - c + n) \rightarrow \Gamma(n - m + 1)$, and all terms on the right-hand side of Eq. (A4) with $n < m$ vanish because the gamma function in the denominator diverges. Then if $n - m = q$, Eq. (A4) becomes

$$\lim_{c \rightarrow m+1} y^{1-c} \frac{\Phi(a - c + 1, 2 - c; y)}{\Gamma(2 - c)} = \sum_{q=0}^{\infty} \frac{\Gamma(a + q)}{\Gamma(a - m)} \frac{y^2}{q!} \frac{1}{(m + q)!} \quad (\text{A5})$$

If we make use of Eq. (5.9) once again, we can write

$$\lim_{c \rightarrow m+1} y^{1-c} \frac{\Phi(a - c + 1, 2 - c; y)}{\Gamma(2 - c)} = \frac{\Gamma(a)}{\Gamma(a + 1 - c)\Gamma(c)} \Phi(a, c; y) \quad (\text{A6})$$

Thus the requirement that Ψ remain finite at $\omega = 0$, when $c = 3$, requires that for the second linearly independent solution used to form the Green's function, we choose the Tricomi function

$$\Psi(a, c; y) = \frac{\Gamma(1 - c)}{\Gamma(a - c + 1)} \Phi(a, c; y) + \frac{\Gamma(c - 1)}{\Gamma(a)} y^{1-c} \Phi(a - c + 1, 2 - c; y) \quad (\text{A7})$$

In Eq. (A7), both terms diverge as $c \rightarrow 3$, but from Eq. (A6), one sees that these divergent pieces cancel, with the consequence that the sum remains finite. The limit $\omega \rightarrow 0$ is then achieved without difficulty.

APPENDIX B: EVALUATION OF THE GREEN'S-FUNCTION INTEGRALS

The first integral which enters Eq. (5.15) may be evaluated by developing Φ in Kummer's series:

$$\int_0^{2d} dy y^{[\gamma\xi + (c-3)/2]} e^{-y/2} \Phi(y) = \sum_n \frac{\Gamma(a+n)\Gamma(c)}{\Gamma(c+n)\Gamma(a)} \frac{1}{n!} \int_0^{2d} dy y^{[\gamma\xi + (c-3)/2+n]} e^{-y/2} \quad (\text{B1})$$

To simplify the notation, let $\gamma\xi + \frac{1}{2}(c - 3) + n = \delta - 1$ for the moment. Then let $t = y/2$ to find

$$\frac{1}{2^\delta} \int_0^{2d} dy y^{\delta-1} e^{-y/2} = \int_0^d t^{\delta-1} e^{-t} dt \quad (\text{B2})$$

The right-hand side of Eq. (B2) is the incomplete gamma function $\gamma(\delta, 2d)$ which may be expressed in terms of the Φ functions by the relation^{26,27}

$$\gamma(\delta, x) = \frac{x^\delta}{\delta} \Phi(\delta, \delta + 1; -x) \quad (\text{B3})$$

Upon making use of Kummer's transformation^{26,27}

$$\Phi(a, c; x) = e^x \Phi(c - a; c; -x) \quad (\text{B4})$$

we obtain

$$\int_0^{2d} y^{\delta-1} e^{-y/2} dy = (2d)^\delta \frac{e^{-d}}{\delta} \Phi(1, \delta + 1; d) \quad (\text{B5})$$

which, when substituted into Eq. (B1) gives

$$\int_0^{2d} dy y^{\gamma\xi + (c-3)/2} e^{-y/2} = e^{-d} \frac{\Gamma(c)}{\Gamma(a)} \sum_{n=0}^{\infty} \frac{\Gamma(a+n)}{(c+n)n!} \frac{(2d)^{[\gamma\xi + (c-3)/2+n+1]}}{\gamma\xi + (c-3)/2+n+1} \Phi(1, n+1; d) \quad (\text{B6})$$

Equation (B1) in combination with Eq. (B6) give the first integral in Eq. (5.15) in terms of a series expansion in Φ functions.

The second integral which enters Eq. (5.15) is

$$I = \int_0^{2d} dy y^{[\gamma\xi + (c-3)/2]} e^{-y/2} \Psi(y) \int_0^y dy' y'^{[\gamma\xi + (c-3)/2]} e^{-y'/2} \Phi(y') \quad (\text{B7})$$

The integral on y' has a form identical to that in Eq. (B1), and which we may have already calculated, provided the upper limit $2d$ of the integral there is replaced by y . Thus with the explicit form for $\Psi(y)$ inserted, we have

$$I = \sum_{n=0}^{\infty} \frac{\Gamma(a+n)}{\Gamma(c+n)} \frac{\Gamma(c)}{\Gamma(a)} \frac{1}{n!} \int_0^{2d} dy y^{2[\gamma\xi+(c-3)/2]+n+1} e^{-y} \frac{\Phi(1, \gamma\xi+(c-1)/2+n+1, y/2)}{\gamma\xi+(c-1)/2+n} \times \left[\frac{\Gamma(1-c)}{\Gamma(a-c+1)} \Phi(a, c; y) + \frac{\Gamma(c-1)}{\Gamma(a)} y^{1-c} \Phi(a-c+1, 2-c; -y) \right]. \tag{B8}$$

Once again, if we expand $\Phi(1, \gamma\xi+(c-1)/2+n+1; y/2)$ according to Eq. (5.9), the integral in Eq. (B8) can be reduced to a sequence of integrals each of which has the form of Eq. (B1). We then find

$$I = \sum_{n=0}^{\infty} \frac{\Gamma(a+n)}{\Gamma(c+n)} \frac{\Gamma(c)}{\Gamma(a)} \frac{1}{n!} \times \sum_{m=0}^{\infty} \frac{e^{-2d} \Gamma(\gamma\xi+(c-1)/2+n)}{\Gamma(\gamma\xi+(c-1)/2+n+m+1)} \frac{\Gamma(c)\Gamma(1-c)}{\Gamma(a)\Gamma(a-c+1)} \times d^m (2d)^{2\gamma\xi+n} \left[\sum_{p=0}^{\infty} \frac{(2d)^p}{p!} (2d)^{c-1} \frac{\Gamma(a+p)}{\Gamma(c+p)} \times \frac{\Phi(1, 2\gamma\xi+c+n+m+p; 2d)}{2\gamma\xi+c+n+m+p-1} - \sum_{p=0}^{\infty} \frac{(2d)^p}{p!} \frac{\Gamma(a-c+p+1)}{\Gamma(2-c+p)} \frac{\Phi(1, 2\gamma\xi+n+m+p+1; 2d)}{2\gamma\xi+n+m+p} \right]. \tag{B9}$$

In Eq. (B9), the recursion relation for the gamma function has been used to write

$$\Gamma(c-1)\Gamma(2-c) = -\Gamma(c)\Gamma(1-c). \tag{B10}$$

It is then straightforward to derive Eq. (5.16) from Eqs. (B1), (B7), and (B9) in which the terms $p=0$ and $p=1$ are separated from the other terms of the second series in p entering this equation.

In the particular case $\omega=0$, the parameter c is an integer: $c=3$, so the standard form of the ψ function in Eq. (5.10) breaks down. However, Whittaker and Watson have defined an integral representation of the Ψ function which may be used to extend its definition to $c=3$. One has²⁷

$$\Psi(a, c; y) = \frac{1}{2\pi i} \int_{\gamma-i\infty}^{\gamma+i\infty} \frac{\Gamma(a+s)\Gamma(-s)\Gamma(1-c-s)y^s}{\Gamma(a)\Gamma(a-c+1)} y^s ds, \tag{B11}$$

which remains well defined when c is an integer. The residues at the second-order poles which occur when c is an integer have been evaluated by Erdelyi *et al.*²⁶ In our particular case, the result reads

$$\Psi(a, 3; y) = \frac{1}{\Gamma(a)y^2} + \frac{2-a}{\Gamma(a)} \frac{1}{y} - \frac{1}{2\Gamma(a-2)} \Phi(a; 3; y) \ln y - \frac{1}{\Gamma(a)\Gamma(a-r)} \sum_{r=0}^{\infty} [\tilde{\psi}(a+r) - \tilde{\psi}(1+r) - \tilde{\psi}(3+r)] \frac{\Gamma(a+r)}{(r+2)!r!} y^r, \tag{B12}$$

where $\tilde{\psi}$ is the digamma function. The only new integral which enters Eq. (B8) when Eq. (B12) is substituted to Eq. (5.10) into the parenthesis in Eq. (B8) comes from the logarithmic term. This can be written

$$J = \int_0^{2d} y^{2\gamma\xi+n+m+1} \Phi(a, 3; y) \ln(y) e^{-y} dy. \tag{B13}$$

If we develop Φ and e^{-y} in a Taylor series in y , then integrate J by parts, we find

$$J = \sum_{p=0}^{\infty} \frac{\Gamma(a+p)}{\Gamma(a)} \frac{2}{(p+2)!p!} (2d)^{2\gamma\xi+n+m+p+2} \times \left[\ln(2d) \left[\sum_{q=0}^{\infty} \frac{(-1)^q (2d)^q}{q!(2\gamma\xi+n+m+p+q+2)} \right] - \sum_{q=0}^{\infty} \frac{(-1)^q (2d)^q}{q!(2\gamma\xi+n+m+p+q+2)^2} \right] \tag{B14}$$

According to Eq. (5.9)

$$\sum_q \frac{(-1)^q (2d)^q}{q!(\alpha+q+2)} = \frac{\Phi(\alpha+2, \alpha+3; -2d)}{\alpha+2} \tag{B15}$$

and, taking Eq. (B4) into account, we can write

$$\sum_{q=0}^{\infty} \frac{(-1)^q (2d)^q}{q! (2\gamma\xi + n + m + p + q + 2)} = \frac{e^{-2d} \Phi(1, 2\gamma\xi + n + m + p + 3; 2d)}{2\gamma\xi + n + m + p + 2} \quad (\text{B16})$$

which determines the coefficient of $(2d)$ in Eq. (B14). Then it is a matter of straightforward algebra to derive Eq. (5.21) from Eqs. (B1), (B6), and (B14).

APPENDIX C: COMMENTS ON THE NUMERICAL PROCEDURES

In this appendix, we comment briefly on the numerical procedures we have used, since similar series expansions are encountered in other surface problems, where surface inhomogeneities are modeled.²³

The Γ and $\tilde{\Psi}$ functions in Eqs. (5.16) and (5.21) have been calculated for a particular set of the indices n , m , and p by use of the Stirling formula:

$$\ln \Gamma(z) = (z - \frac{1}{2}) \ln z - z + \frac{1}{2} \ln(2\pi) + \sum_{m=1}^{\infty} B_{2m} \frac{z^{1-2m}}{2m(2m-1)} \quad (\text{C1})$$

and

$$\tilde{\Psi}(z) = \ln z - \frac{1}{2z} + \sum_{m=1}^{\infty} B_{2m} \frac{z^{-2m}}{2m} \quad (\text{C2})$$

The coefficients B_{2m} are Bernoulli numbers, and are tabulated.²⁸ The series have been truncated at $m=10$ to compute both functions, and double precision has been used for $|z| > 6$, with $\text{Re} z > 0$. If $|z| < 6$, we have used the recursion relations

$$\Gamma(1+z) = z\Gamma(z), \quad \tilde{\Psi}(1+z) = \frac{1}{z} + \tilde{\Psi}(z), \quad (\text{C3})$$

to map the calculation of the functions into the domain $|z| > 6$. If $\text{Re} z < 0$, we use the functional relations

$$\tilde{\Psi}(z) - \tilde{\Psi}(1-z) = -\pi \cot(\pi z) \quad (\text{C4})$$

and

$$\Gamma(z)\Gamma(-z) = -\frac{\pi}{\sin(\pi z)}, \quad (\text{C5})$$

so in fact the series are always evaluated in the domain $\text{Re} z > 0$, $|z| > 6$, where the series representations are very accurate. The other terms of the series in Eqs. (5.16) and (5.21) are deduced from the recursion relations in Eq. (C3) supplemented by the following equation:

$$\Phi(a, c; z) = \frac{z}{c} \Phi(a, c+1; z). \quad (\text{C6})$$

Even though the series we must evaluate involves sums over three indices, the convergence is very fast. The reason is that all the terms which depend on the gamma functions are decreasing functions of the indices n , m , and p while $\Phi(a, c; z) \rightarrow 1$ when $C \rightarrow \infty$. So the series converge more rapidly than $\sum_n (2d)^n / n! = \exp(2d)$. Suppose we consider the series just stated, and imagine that both n and $2d$ are large compared to unity. Then use of Stirling's formula gives

$$\frac{(2d)^n}{n!} \cong \frac{n^{1/2}}{(2\pi)^{1/2}} \left[\frac{2ed}{n} \right]^n \quad (\text{C7})$$

The expression is a maximum for $n=2d$, and for this value of n , $(2d)^n n! \cong \exp(2d)(d/\pi)^{1/2}$. This result and the earlier remarks in this paragraph show that the series in the text may be evaluated to better than one part in 10^5 if the series is truncated at $n=m=p=N$ defined by

$$\left[\frac{2ed}{N} \right]^n \left[\frac{N}{2d} \right]^{1/2} e^{-2d} = 10^{-5}. \quad (\text{C8})$$

The value of N for each value of d investigated has been computed from Eq. (C8). The largest value of N encountered is for $Q_0=1$ and $T=T_c$, and this is $N=32$. The amount of computer time required for this task is very small.

*Permanent address: Centre National de la Recherche Scientifique, 1 place A. Briand 92190 Meudon, France.

¹See D. L. Mills and K. R. Subbaswamy, in *Progress in Optics*, edited by E. Wolf (North-Holland, Amsterdam, 1981), Vol. XIX, p. 47.

²S. Ushioda, in *Progress in Optics*, Ref. 1, p. 141.

³See J. P. Jackson, *Classical Electrodynamics* (Wiley, New York, 1962), p. 220.

⁴J. G. Dil and N. C. J. van Hijningen, *Phys. Rev. B* **22**, 5924 (1980).

⁵Rather than use the "one-bounce" geometry as illustrat-

ed in our Fig. 1, Stegeman has pointed out that the thin-film-integrated-optics geometry employed in a study of phonons in thin films [N. L. Rowell and G. I. Stegeman, *Phys. Rev. Lett.* **41**, 970 (1978)] offers numerous advantages, G. I. Stegeman (private communication).

⁶K. Miyano, *Phys. Rev. Lett.* **43**, 51 (1979).

⁷U. T. Höchli and H. Rohrer, *Phys. Rev. Lett.* **48**, 188 (1982).

⁸P. G. de Gennes, *The Physics of Liquid Crystals*, (Oxford University Press, Oxford, 1974).

- ⁹D. Balzarini, Phys. Rev. Lett. 25, 914 (1970).
- ¹⁰D. L. Mills and A. A. Maradudin, Phys. Rev. B 12, 2943 (1975).
- ¹¹P. G. de Gennes, Mol. Cryst. Liq. Cryst. 12, 193 (1971).
- ¹²Ping Sheng, Phys. Rev. Lett. 37, 1059 (1976).
- ¹³J. L. Ericksen, Arch. Ration. Mech. Anal. 10, 189 (1962).
- ¹⁴P. G. de Gennes, Phys. Lett. 30A, 454 (1969).
- ¹⁵J. D. Lister and T. W. J. Stensen, Phys. Rev. Lett. 25, 503 (1970).
- ¹⁶See, for example, D. N. Zubarev, Usp. Fiz. Nauk 71, 71 (1960) [Sov. Phys.—Usp. 3, 320 (1960)].
- ¹⁷See discussions in B. Friedman, *Principles and Techniques of Applied Mathematics* (Wiley, New York, 1956), Chap. 8.
- ¹⁸M. C. Oliveros and D. R. Tilley, J. Phys. (in press).
- ¹⁹E. T. Whittaker, Bull. Am. Math. Soc. 10, 185 (1904).
- ²⁰For a review, see, for example, F. G. Tricomi, *Funzioni Ipergeometriche Confluenti* (Edizioni Cremonese, Roma, Italy, 1954).
- ²¹P. M. Morse, Phys. Rev. 34, 57 (1929).
- ²²H. B. Rosenstock, Phys. Rev. B 9, 1963 (1974).
- ²³H. S. Jarrett, J. Appl. Phys. 52, 4681 (1981). According to Eq. (6.12) of our paper, the junctions $N_1(\epsilon)$ and $N_2(\epsilon)$ defined in Eq. 12 of the paper of Jarrett could be read $\Phi(\nu/2, 1/2; \epsilon^2/2)$ and $\Psi(\nu/2, 1/2; \epsilon^2/2)$, with $\nu = 1 + \tau_i/\tau_R$.
- ²⁴M. Buchholz, *Die Konfluente Hypergeometrische Funktion* (Springer, Berlin, 1953). Note that with respect to the usual definition of $E_\nu^{(1)}$ given by Buckholz, we have replaced Φ by Ψ in Eq. (6.12), for homogeneity purposes with Appendix B of our present paper.
- ²⁵E. Schrödinger, Ann. Phys. (Leipzig) 80, 483 (1926).
- ²⁶A. Erdelyi, W. Magnus Oberhettinger, and F. G. Tricomi, *Higher Transcendental Functions* (McGraw-Hill, New York 1953), Vol. 1, p. 202.
- ²⁷E. T. Whittaker and G. N. Watson, *A Course of Modern Analysis* (Cambridge University Press, Cambridge, 1927), Sec. 16.4.
- ²⁸See, for example, *Handbook of Mathematical Functions*, edited by M. Abramowitz and I. A. Stegun (Dover, New York, 1970), p. 180.